RESEARCH ARTICLE

# Binding of Alphaherpesvirus Glycoprotein H to Surface $\alpha_4\beta_1$-Integrins Activates Calcium-Signaling Pathways and Induces Phosphatidylserine Exposure on the Plasma Membrane

**Walid Azab,[a] Andrea Gramatica,[b] Andreas Herrmann,[b] Nikolaus Osterrieder[a]**

Institut für Virologie, Robert von Ostertag-Haus, Zentrum für Infektionsmedizin, Freie Universität Berlin, Berlin, Germany[a]; Institut für Biologie/Molekulare Biophysik, Humboldt Universität zu Berlin, Berlin, Germany[b]

**ABSTRACT** **Intracellular signaling connected to integrin activation is known to induce cytoplasmic $Ca^{2+}$ release, which in turn mediates a number of downstream signals. The cellular entry pathways of two closely related alphaherpesviruses, equine herpesviruses 1 and 4 (EHV-1 and EHV-4), are differentially regulated with respect to the requirement of interaction of glycoprotein H (gH) with $\alpha_4\beta_1$-integrins. We show here that binding of EHV-1, but not EHV-4, to target cells resulted in a rapid and significant increase in cytosolic $Ca^{2+}$ levels. EHV-1 expressing EHV-4 gH (gH4) in lieu of authentic gH1 failed to induce $Ca^{2+}$ release, while EHV-4 with gH1 triggered significant $Ca^{2+}$ release. Blocking the interaction between gH1 and $\alpha_4\beta_1$-integrins, inhibiting phospholipase C (PLC) activation, or blocking binding of inositol 1,4,5-triphosphate ($IP_3$) to its receptor on the endoplasmic reticulum (ER) abrogated $Ca^{2+}$ release. Interestingly, phosphatidylserine (PS) was exposed on the plasma membrane in response to cytosolic calcium increase after EHV-1 binding through a scramblase-dependent mechanism. Inhibition of both $Ca^{2+}$ release from the ER and scramblase activation blocked PS scrambling and redirected virus entry to the endocytic pathway, indicating that PS may play a role in facilitating virus entry directly at the plasma membrane.**

**IMPORTANCE** **Herpesviruses are a large family of enveloped viruses that infect a wide range of hosts, causing a variety of diseases. These viruses have developed a number of strategies for successful entry into different cell types. We and others have shown that alphaherpesviruses, including EHV-1 and herpes simplex virus 1 (HSV-1), can route their entry pathway and do so by manipulation of cell signaling cascades to ensure viral genome delivery to nuclei. We show here that the interaction between EHV-1 gH and cellular $\alpha_4\beta_1$-integrins is necessary to induce emptying of ER calcium stores, which induces phosphatidylserine exposure on the plasma membrane through a scramblase-dependent mechanism. This change in lipid asymmetry facilitates virus entry and might help fusion of the viral envelope at the plasma membrane. These findings will help to advance our understanding of herpesvirus entry mechanism and may facilitate the development of novel drugs that can be implemented for prevention of infection and disease.**

**Received** 14 September 2015 **Accepted** 21 September 2015 **Published** 20 October 2015

**Citation** Azab W, Gramatica A, Herrmann A, Osterrieder N. 2015. Binding of alphaherpesvirus glycoprotein H to surface $\alpha_4\beta_1$-integrins activates calcium-signaling pathways and induces phosphatidylserine exposure on the plasma membrane. mBio 6(5):e01552-15. doi:10.1128/mBio.01552-15.

**Invited Editor** Roselyn J. Eisenberg, University of Pennsylvania **Editor** Glen Nemerow, Scripps Research Institute



Address correspondence to Walid Azab, wfazab@zedat.fu-berlin.de.

Entry of alphaherpesviruses is a complex process, which requires the concerted activity of different envelope glycoproteins as well as different cellular receptors and coreceptors (1–5). Binding of viruses to cellular receptors often activates intracellular signaling pathways that in turn facilitate virus uptake. Productive entry of different alphaherpesviruses has been shown to occur through different pathways. Depending mainly on the cell type, virus penetration is executed either through fusion at the plasma membrane (6–10), endocytosis (7, 11–16), or phagocytosis-like macropinocytosis (17). For herpes simplex virus 1 (HSV-1), it has been shown that $\alpha_V\beta_3$-integrins serve as a routing factor that directs the virus to a pathway that is dependent on lipid microdomains, dynamin-II, and acidification of endosomes (18). Recently, we have identified cellular and viral routing factors that determine entry of equine herpesviruses 1 and 4 (EHV-1 and -4), members of the *Alphaherpesvirinae* subfamily (19, 20). Although both viruses bind the same entry receptor, major histocompatibility class I (MHC-I), through glycoprotein D (gD) (3, 5, 21), they follow different entry pathways: EHV-4 entry proceeds via a caveolin/raft-dependent endocytic pathway, while EHV-1 enters cells through either direct fusion with the plasma membrane or endocytosis (22). The decision for one of the two pathways is mainly dependent on the interaction between viral glycoprotein H (gH) and cellular $\alpha_4\beta_1$-integrins that function as a coreceptor (22), but the molecular mechanisms that determine routing are unknown. One possibility, among others, is that differential signaling following virus attachment determines which pathway is utilized. The modulation of intracellular signaling and its effects on the route of entry of viruses is supported by previous studies, which showed that early virus-cell interactions at the plasma membrane direct viruses to specific cellular compartments (23–25).

Integrins are transmembrane heterodimers that can initiate a signaling cascade upon interaction with their specific ligands that results in the phosphorylation of tyrosine residues of intracellular proteins, including paxillin, tensin, focal adhesion kinase, and mitogen-activated protein kinases (26–29). Previous studies also showed that the engagement of $\alpha_4\beta_1$-integrins resulted in phospholipase C (PLC) activation and an increase of cytosolic $Ca^{2+}$ concentrations (27, 30). Activation of PLC results in the hydrolysis of phosphatidylinositol 4,5-bisphosphate ($PIP_2$) to generate two intracellular messengers: inositol 1,4,5-triphosphate ($IP_3$), which can trigger release of $Ca^{2+}$ from intracellular stores (e.g., the endoplasmic reticulum [ER]), and diacylglycerol (DAG), which is responsible for the activation of different downstream proteins (e.g., protein kinase C [PKC]) (28, 31). $IP_3$ diffuses through the cytoplasm and binds to the $IP_3$ receptor ($IP_3R$) localized on the cytoplasmic side of the ER, which in turn mobilizes ER-resident (stored) $Ca^{2+}$ (31, 32).

$Ca^{2+}$ is one of the most prominent and universal carriers of signals and acts as a second messenger in mammalian cells. $Ca^{2+}$ is known to modulate a number of steps during virus replication, from virus entry to virion maturation and release (33, 34). Free cytosolic $Ca^{2+}$ is maintained in concentrations of approximately 100 nM. The concentration of stored $Ca^{2+}$, mainly in the ER, is maintained at several hundred micromolar, whereas extracellular $Ca^{2+}$ concentrations can reach the millimolar range (33). Thus, cells tightly control intracellular $Ca^{2+}$ homeostasis to avoid acute gigantic fluctuations (35). The increase in intracellular $Ca^{2+}$ is usually triggered by specific stimuli such as ligand-receptor interactions on the cell surface that often converge on PLC activation and $IP_3$-$IP_3R$ interaction (33, 36). Viruses have adopted strategies to hijack $Ca^{2+}$-mediated signaling events to promote entry and/or replication (33). Previous reports have shown that exposure of epithelial and neuronal cells to either HSV-1 or HSV-2 results in a rapid and transient increase in cytosolic $Ca^{2+}$. As described above, the process requires activation of PLC and subsequent $IP_3$-$IP_3R$ interaction (37, 38).

We previously reported that the interaction between viral gH and cellular integrins plays a decisive role for EHV-1 and EHV-4 entry. We suggested that differential signaling may determine the entry pathway (22). In this study, we show an increase in cytosolic $Ca^{2+}$ concentration upon infection with EHV-1 and characterize the cellular factors required for this augmentation. In particular, we studied factors that are potentially associated with changes of the plasma membrane affecting the entry pathway, such as the level of the virus entry receptor MHC-I and its distribution on the cell surface, the actin cytoskeleton, and the lipid composition of the exoplasmic lipid layer of the plasma membrane.

## RESULTS

**EHV-1 binding triggers a rapid increase in cytosolic $Ca^{2+}$.** We have shown that EHV-1 and EHV-4 use different entry pathways during infection of epithelial cells (22). However, the intracellular signaling cascades that are initiated during entry of either virus are still unknown. To evaluate whether exposure of equine cells to EHV-1 or EHV-4 results in an increase in cytosolic $Ca^{2+}$, concentrations of cytosolic $Ca^{2+}$ were monitored using an epifluorescence microscope using the membrane-permeable $Ca^{2+}$ fluorophore Fura-2AM. Fura-2 is a fluorescent dye that binds to free cytosolic $Ca^{2+}$; an increase in Fura-2 fluorescence indicates an increase of the cytosolic $Ca^{2+}$ concentration.

Equine dermal (ED) cells were first loaded with Fura-2 and then exposed to $Ca^{2+}$-free medium, ionomycin (plus 3 mM $CaCl_2$), EHV-1, or EHV-4. Live-cell imaging revealed that addition of EHV-1 to ED cells resulted in a rapid increase of cytosolic $Ca^{2+}$ concentrations as measured by Fura-2 fluorescence. This increase peaked within 2 min and lasted to the end of the capture period (10 min) (Fig. 1A; see Movie S1 in the supplemental material). Addition of the calcium ionophore ionomycin also resulted in a strong and rapid increase in cytosolic $Ca^{2+}$ (Fig. 1A). In contrast, addition of EHV-4 or $Ca^{2+}$-free medium had no effect on cytosolic $Ca^{2+}$ levels (Fig. 1A; see Movie S2 in the supplemental material). The mean change in cytosolic $Ca^{2+}$ peaks obtained for EHV-1 was significant compared to that for EHV-4 or $Ca^{2+}$-free medium (Fig. 1B).

**Cytosolic $Ca^{2+}$ increase is dependent on gH–$\alpha_4\beta_1$-integrin interaction.** In a previous study, we showed that viral gH and cellular $\alpha_4\beta_1$-integrins play an important role during EHV-1 and EHV-4 entry and that both can act as a routing factor capable of altering the entry pathways of the viruses (22). Following up on these results, we explored the possibility that interaction between gH and $\alpha_4\beta_1$-integrins may trigger release of $Ca^{2+}$ from intracellular stores. Based on live-cell-imaging measurements, we concluded that, in contrast to parental EHV-1, EHV-1 bearing gH4 (EHV-1gH4) was unable to trigger an increase of cytosolic $Ca^{2+}$. On the other hand, EHV-4 expressing and having in its envelope gH1 (EHV-4gH1) induced a significant increase of cytosolic $Ca^{2+}$ (Fig. 2A). It is important to note that only EHV-1 gH has an integrin-binding motif, serine-aspartate-isoleucine (SDI), that mediates binding to $\alpha_4\beta_1$-integrins. EHV-4 gH specifies an alanine-aspartate-isoleucine (ADI) motif that cannot mediate integrin binding (39). Addition of EHV-1gH$^{S440A}$, an EHV-1 mutant in which the $\alpha_4\beta_1$-integrin binding motif SDI was mutated to ADI, had no effect on cytosolic $Ca^{2+}$ levels (see Movie S3 in the supplemental material). From the experiments, we concluded that gH plays a role in increasing cytosolic $Ca^{2+}$ levels through a mechanism that is dependent on the interaction of gH with integrins expressed on the cell surface.

To further elucidate the role of integrins, we analyzed the increase of cytosolic $Ca^{2+}$ after blocking the interaction between viral gH and cell surface integrins. First, Fura-2-loaded cells were incubated with the anti-$\alpha_4\beta_1$-integrin monoclonal antibody (MAb) P4C2 for 1 h before exposure to either EHV-1 or EHV-4gH1. Although both viruses were still able to bind to cells, addition of either virus did not have a significant effect on the resting cytosolic $Ca^{2+}$ (Fig. 2B). Similarly, incubation of the viruses with soluble $\alpha_4\beta_1$-integrins before infection did not induce any increase in cytosolic $Ca^{2+}$ (Fig. 2C). We concluded, therefore, that $\alpha_4\beta_1$-integrins play a role in increasing cytosolic $Ca^{2+}$ levels after exposure to viruses that have an integrin-binding motif present in gH, which indicates that the interaction between gH and integrins may trigger $Ca^{2+}$-signaling pathways.

Previous reports have shown that heat inactivation of herpesviruses is similar to UV light inactivation and that such viruses were devoid of measurable infectivity (40). Similarly, we found that heat-inactivated EHV-1 was also unable to establish infection and that enhanced green fluorescent protein (eGFP), under the control of the immediate early human cytomegalovirus (HCMV) promoter, was not expressed (see Fig. S1A in the supplemental material). However, the virus was still able to bind to the cells but to a lesser extent than the parental virus (see Fig. S1B). Exposure of

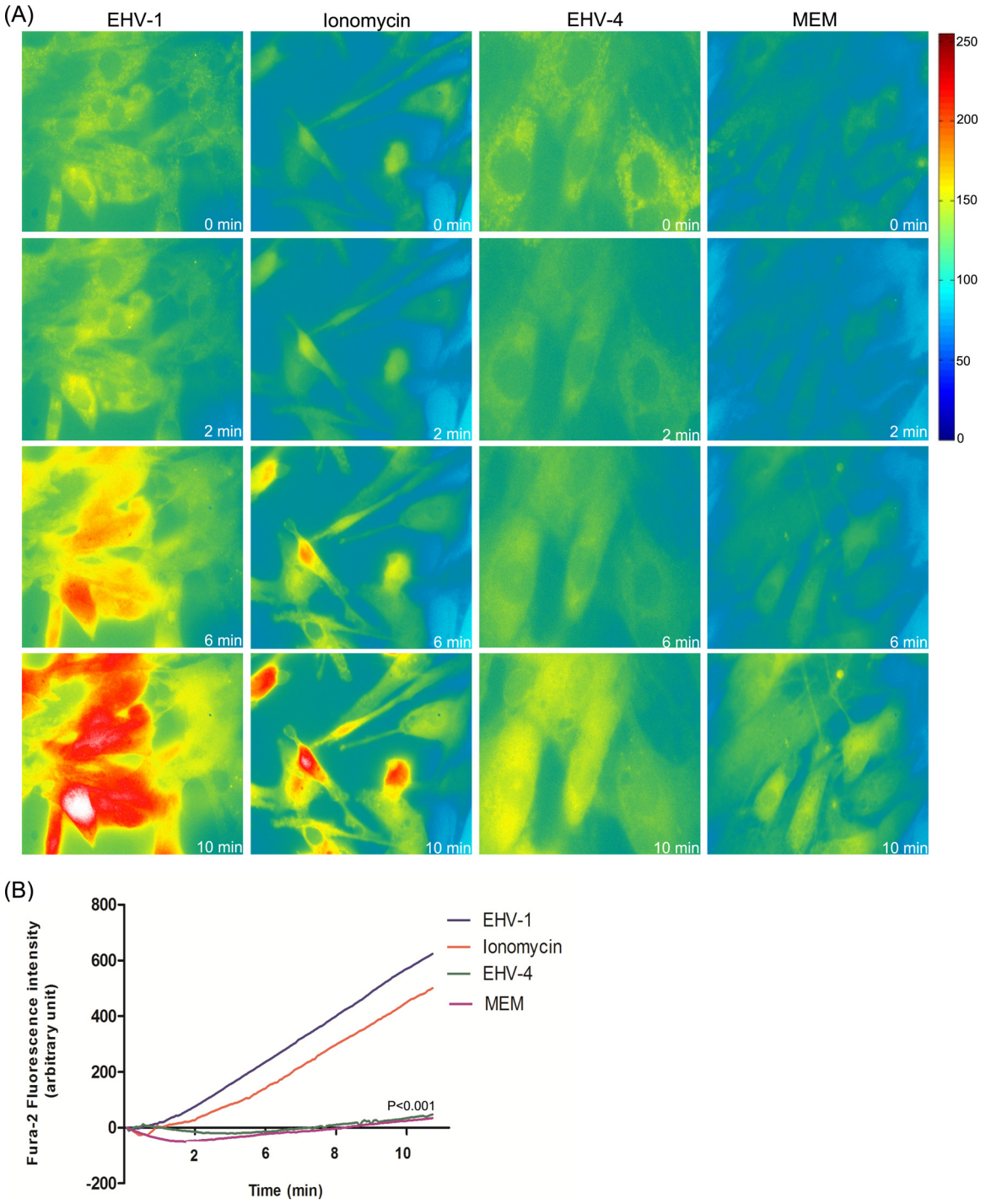


**FIG 1** EHV-1 triggers the increase of cytosolic $Ca^{2+}$. (A) ED cells were loaded with Fura-2AM, and live fluorescent images were taken every 5 s prior to and following the addition of EHV-1, ionomycin, EHV-4, or $Ca^{2+}$-free medium (MEM) at time point 50 s. Shown is one representative image captured at each of the indicated time points. (B) The curves shown refer to the average of three independent experiments of fluorescence intensities of Fura-2AM versus time of excited ED cells being exposed to EHV-1, EHV-4, ionomycin, or MEM. $P < 0.001$ indicates a significant difference between EHV-1 and ionomycin compared to EHV-4 and MEM.

Fura-2-loaded cells to heat-inactivated virus clearly showed that virus binding was able to trigger the increase of cytosolic $Ca^{2+}$ with kinetics and magnitudes comparable to those of the parental virus (Fig. 3).

**Inhibition of PLC and $IP_3R$ abrogates EHV-1-induced cytosolic $Ca^{2+}$ increase.** Cytosolic $Ca^{2+}$ increase is often initiated through signaling molecules that are activated in response to a ligand-receptor interaction on the cell surface (41). In order to

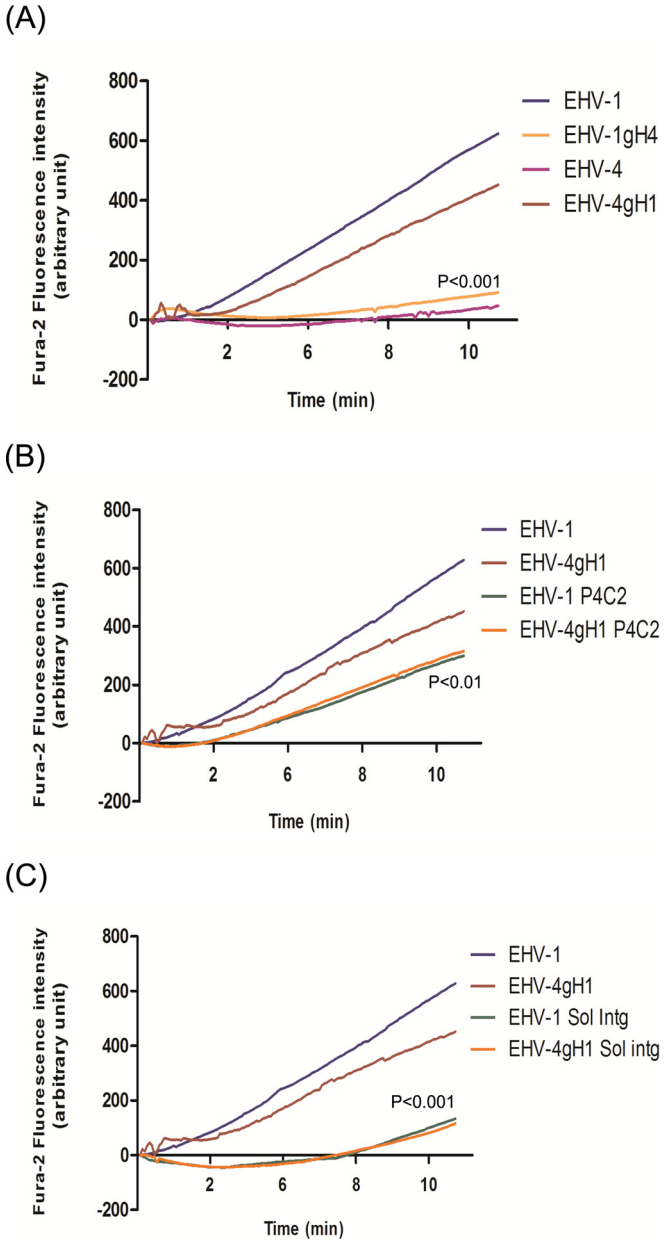


**FIG 2** EHV-1 gH and cellular $\alpha_4\beta_1$-integrin mediate cytosolic $Ca^{2+}$ increase during virus entry. (A) ED cells were loaded with the $Ca^{2+}$ indicator Fura-2AM and exposed to EHV-1, EHV-4, EHV-1gH4, or EHV-4gH1. (B) ED cells were incubated with 20 $\mu$g/ml of anti–$\alpha_4\beta_1$-integrin MAb P4C2 for 1 h at 37°C. After washing, cells were loaded with Fura-2AM and exposed to EHV-1 and EHV-4gH1. (C) EHV-1 and EHV-4gH1 were incubated with soluble $\alpha_4\beta_1$-integrin for 1 h at 37°C. The cells were loaded with Fura-2AM and exposed to the viruses. Changes in cytosolic $Ca^{2+}$ levels were monitored using epifluorescence microscopy. Viruses were added at 50-s time point. The average from three independent experiments of fluorescence intensities of Fura-2AM versus time of exposure of ED cells to the viruses is shown. (A) $P < 0.001$ indicates a significant difference between EHV-1gH4 and EHV-4gH1 compared to parental EHV-1 and EHV-4, respectively. (B) $P < 0.01$ indicates a significant difference between EHV-1 and EHV-4gH1 viruses in the presence or absence of the integrin antibodies. (C) $P < 0.001$ indicates a significant difference between EHV-1 and EHV-4gH1 viruses in the presence or absence of soluble $\alpha_4\beta_1$-integrin (Sol intg).

determine whether the observed increase of cytosolic $Ca^{2+}$ was mediated by the activation of PLC and subsequent binding of $IP_3$ to its cognate receptor $IP_3R$, the effects of (−)-xestospongin C, a specific and potent blocker of $IP_3R$, and U73122, a specific PLC inhibitor, on cytosolic $Ca^{2+}$ levels were investigated. We found that pretreatment of Fura-2-loaded ED cells with U73122 or (−)-xestospongin C abolished the increase of cytosolic $Ca^{2+}$ in response to EHV-1 (Fig. 4) and EHV-4gH1 (Fig. 5). We further showed that the increase in Fura-2 fluorescence started from the perinuclear area, which suggests release of $Ca^{2+}$ from ER stores (see Movie S4 in the supplemental material).

**Blocking $Ca^{2+}$ release reroutes EHV-1 to the endocytic pathway.** Since our data showed that gH1-integrin interaction resulted in a significant increase of cytosolic $Ca^{2+}$, we investigated the route of entry of EHV-1 using various inhibitors. ED cells were incubated with the $Ca^{2+}$ chelator BAPTA-AM [1,2-bis(2-aminophenoxy)ethane-*N*,*N*,*N*′,*N*′-tetraacetic acid tetrakis(acetoxymethyl ester)] or thapsigargin (Table 1) for 1 h before infection with EHV-$1^{RFP}$ (i.e., EHV-1 expressing red fluorescent protein). Colocalization with either caveolin-1 (Cav-1) or clathrin was determined by confocal microscopy using the respective antibodies. Twelve fields were randomly selected, and around 200 individual viruses were counted (Fig. 6G). No significant (approximately 20%) colocalization with either Cav-1 or clathrin was detected in the absence of either inhibitor (Fig. 6A and D). In contrast, approximately 50% of the virus signals were colocalizing with Cav-1 (Fig. 6B and C), but not clathrin (Fig. 6E and F), after inhibiting cytosolic $Ca^{2+}$ increase.

To extend and confirm the results, we conducted a double inhibition infection assay. ED cells were first incubated with different inhibitors, including 2-APB, verapamil, BAPTA-AM, (−)-xestospongin C, U73122, thapsigargin, dynasore, or genistein (Table 1) before infection with EHV-1. In another experiment, the cells were incubated with either dynasore or genistein together with BAPTA-AM, U73122, or thapsigargin and infected with EHV-1. Our results showed that single inhibition with any of the calcium inhibitors or with dynasore and genistein did not have a significant effect on the level of virus infection (Fig. 7A and B). In contrast, double inhibition with either dynasore or genistein together with one of the calcium inhibitors significantly ($P < 0.05$) reduced the number of infected cells (Fig. 7C). We corroborated the dynasore inhibitor experiments using wild-type dynamin (wt-DynII) and dominant-negative dynamin (DynII-K44A), which were kindly provided by Mark A. McNiven (Mayo Clinic, Rochester, MN) (42, 43). We found that the expression of DynII-K44A alone did not significantly inhibit EHV-1 infection compared to wt-DynII. However, addition of BAPTA-AM, U73122, or thapsigargin to DynII-K44A-transfected cells (i.e., forcing the virus into endocytic entry) significantly reduced virus infection as well (see Fig. S2 in the supplemental material).

We concluded from the experiments that $Ca^{2+}$ inhibitors alone do not inhibit virus infection and that blocking of $Ca^{2+}$ release from the ER reroutes the majority of virus particles to the caveolin-endocytic pathway. In contrast, inhibitors targeting viral entry through the endocytic pathway, dynamin-II and tyrosine kinase, together with inhibiting $Ca^{2+}$ release, resulted in a significant reduction of virus infection. In other words, these experiments suggest that the combination of blockade of $Ca^{2+}$ release from the ER and inhibition of endocytosis "shuts both entry doors," the plasma membrane and the endosome.

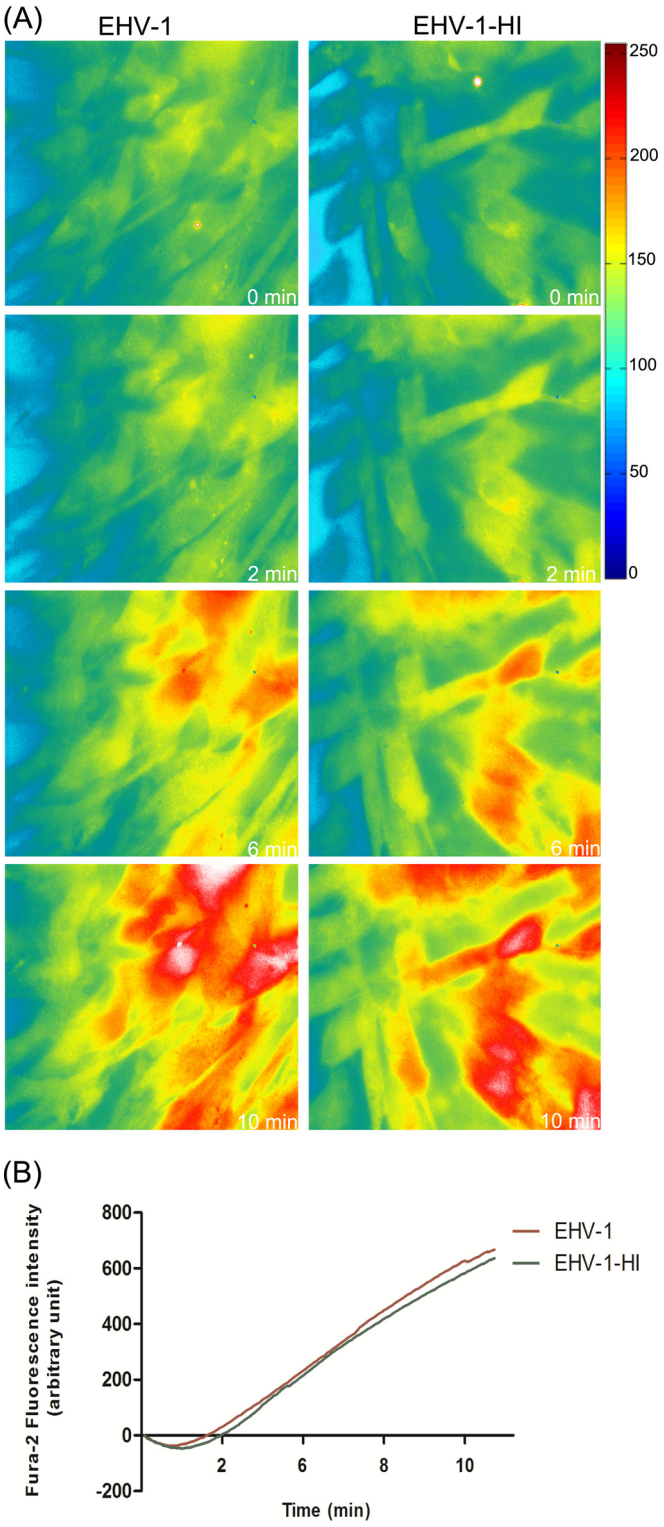


**FIG 3** Inactivated virions trigger cytosolic $Ca^{2+}$ increase. (A) EHV-1 and heat-inactivated EHV-1 (EHV-1-HI) were added to Fura-2AM-loaded ED cells. Live images were monitored and captured at the indicated time points. Viruses were added at the 50-s time point. (B) Fluorescence intensities of Fura-2AM as a function of time after exposure of ED cells to EHV-1 and EHV-1-HI are shown. Data are represented as the averages from 3 independent experiments.

**EHV-1 perturbs lipid asymmetry and exposes phosphatidylserine on the outer leaflet of the plasma membrane.** When EHV-1 was allowed to bind to ED cells for 1 h at 4°C and the temperature was then shifted to 37°C for 5 min, most cells had phosphatidylserine (PS) exposed on the cell surface, as indicated by binding of fluorescent annexin V to the cell surface (Fig. 8A). However, this exposure of PS had no effect on levels of the virus entry receptor (MHC-I) or its distribution on the cell surface (see Fig. S3 in the supplemental material). To further confirm that PS is exposed as a result of virus binding, EHV-1 binding and PS staining were done at 4°C. It was clear that EHV-1 binding was able to induce PS exposure on the cell surface (Fig. 8B). In contrast, EHV-1gH4 did not induce PS exposure on the plasma membrane (Fig. 8A). Blocking cytosolic $Ca^{2+}$ increase in EHV-1-infected cells with BAPTA-AM or thapsigargin as well as interrupting the PLC-$IP_3$R pathway with U73122 blocked PS exposure following EHV-1 infection (Fig. 8C), indicating that this process required intracellular $Ca^{2+}$ mobilization.

Phospholipid scramblases are calcium-dependent proteins that redistribute phospholipids (in particular PS) to the outer leaflet of the plasma membrane (44). To investigate if scramblase is responsible for the PS exposure, EHV-1-infected cells were treated with R5421, a scramblase inhibitor, which blocks $Ca^{2+}$-induced phospholipid scrambling (45–47). EHV-1-induced PS exposure was significantly inhibited by R5421 in a dose-dependent manner (Fig. 8D, left panel), and its potent effect was seen at a concentration of 100 $\mu$M (Fig. 8D, right and left panels). These results suggest that EHV-1-triggered $Ca^{2+}$ release activates a phospholipid scramblase, which exposes PS on the cell surface.

**Blocking PS exposure reroutes EHV-1 to the endocytic pathway.** ED cells were incubated with the scramblase inhibitor R5421 for 1 h before infection with EHV-$1^{RFP}$. We next determined virus colocalization with Cav-1 by confocal microscopy. Twelve fields were randomly selected, and approximately 100 individual viruses were counted (Fig. 9C). As expected, only approximately 20% of EHV-1 particles colocalized with Cav-1 in the absence of the scramblase inhibitor (Fig. 9A). In contrast, around 45% of the virus signals were colocalizing with Cav-1 (Fig. 9B) after inhibiting PS exposure.

Interestingly, virus particles significantly colocalized with the exposed PS on the cell surface (Fig. 9D and F). Incubation of cells with R5421 before infection abrogated PS exposure, and we were barely able to detect any virus colocalization with PS (Fig. 9E). As controls, PS exposure on the surface of mock-infected or staurosporine-treated ED cells is shown (see Fig. S4 in the supplemental material). These data together with the results presented above support the hypothesis that $Ca^{2+}$-dependent PS exposure may enhance EHV-1 entry.

**$Ca^{2+}$ does not modulate the actin cytoskeleton during EHV-1 entry.** There is evidence suggesting that remodeling of the actin cytoskeleton may have a role in regulating fusion of biological membranes (48). During HIV entry, Env-coreceptor interaction stimulates actin filament reorganization and induces cell fusion, aiding in virus entry (49, 50). In addition, it has been shown that the increase in intracellular $Ca^{2+}$ levels leads to actin polymerization (51). Here, we investigated whether $Ca^{2+}$ increase during EHV-1 or EHV-4gH1 entry can affect the actin cytoskeleton. As controls, cells were also infected with EHV-4 or EHV-1gH4. Cells were infected (for either 5 or 60 min), fixed, permeabilized, and stained with Alexa Fluor 568 or 647-labeled phalloidin. We

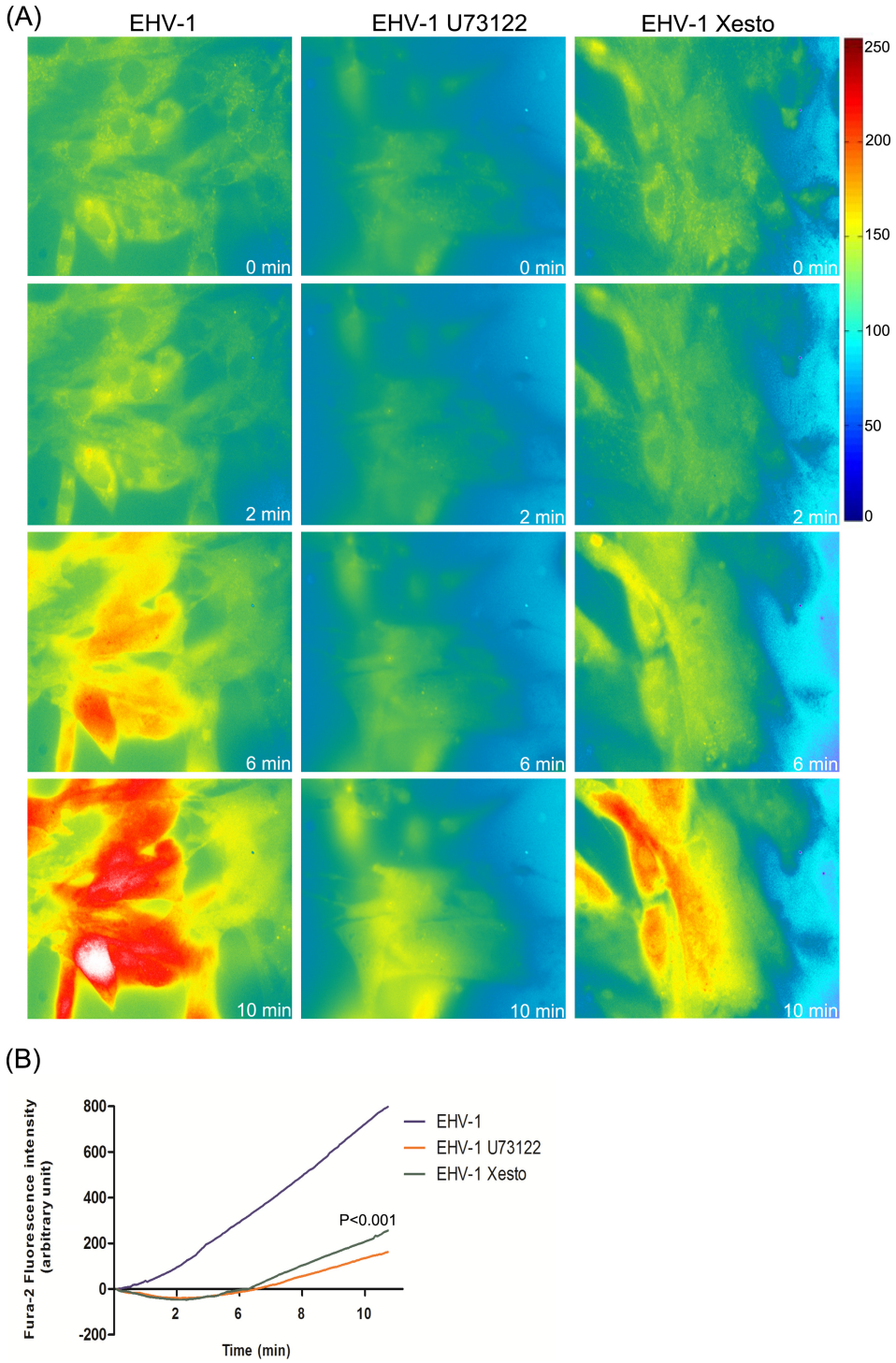


**FIG 4** PLC and $IP_3R$ are required for $Ca^{2+}$ release from ER. (A) ED cells were treated with U73122 or (−)-xestospongin C (Xesto) for 30 to 60 min at 37°C prior to infection. The cells were washed, loaded with Fura-2AM, and exposed to EHV-1. Release of $Ca^{2+}$ was monitored, and images were taken at the indicated time points. Viruses were added at the 50-s time point. (B) Fluorescence intensity of Fura-2AM as a function of time after exposure of ED cells to EHV-1 in the presence or absence of U73122 or (−)-xestospongin C. The lines show averages from 3 independent experiments. $P < 0.001$ indicates a significant difference between EHV-1 in the presence and absence of the used inhibitors.

were unable to observe any significant difference in actin polymerization (see Fig. S5A in the supplemental material) or reorganization (see Fig. S5B) at the time of dramatic increase of cytosolic $Ca^{2+}$ (i.e., within 2 min after addition of virus to cells). However, after 1 h of infection, we found a reduction of actin filaments after infection with any of the viruses (see Fig. S5A). We concluded that actin was depolymerized as a consequence of virus infection at later time points but likely through a $Ca^{2+}$-independent mecha-

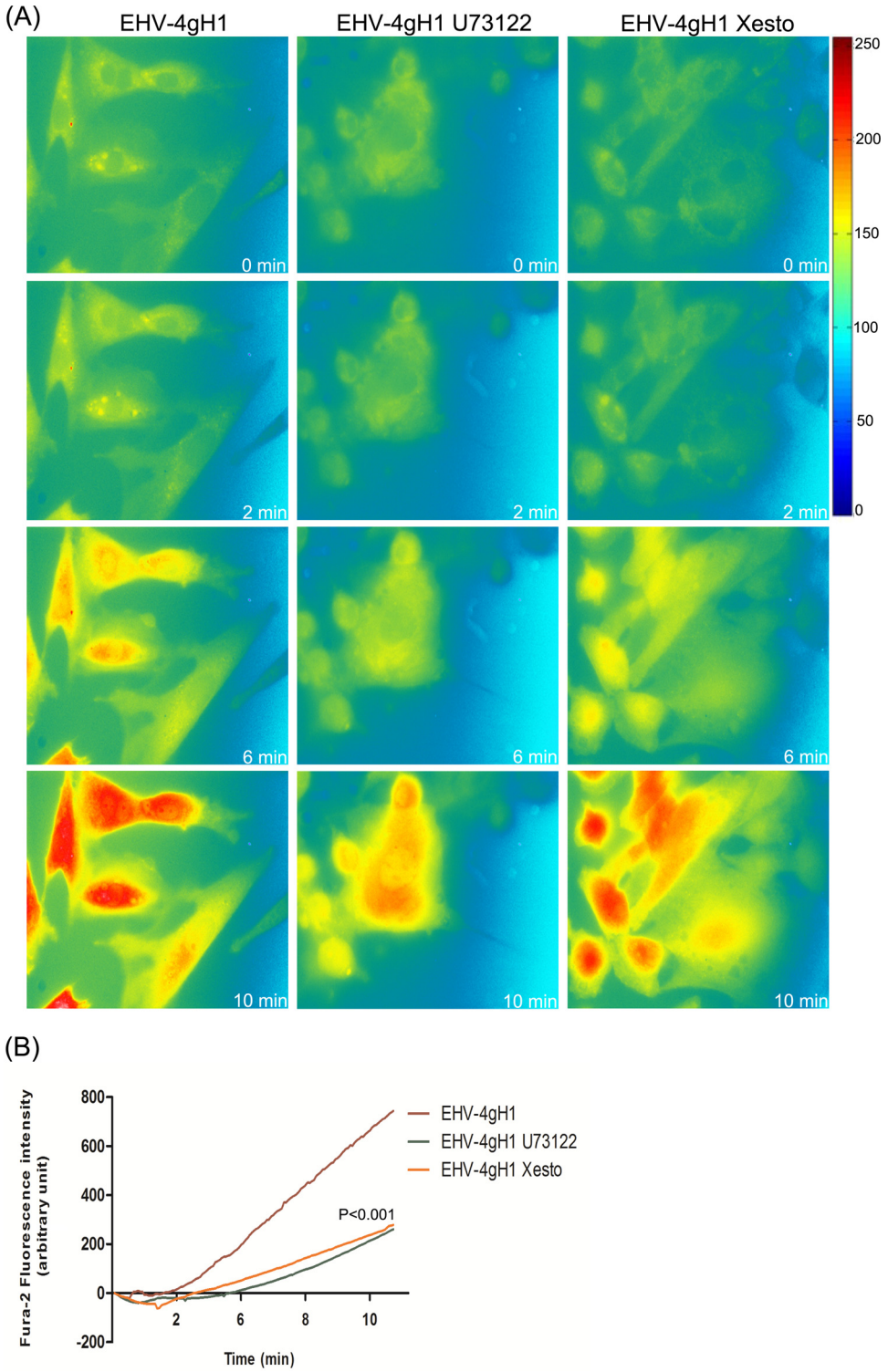


**FIG 5** EHV-1 gH activates PLC-$IP_3$R to induce $Ca^{2+}$ release from ER. (A) ED cells were treated with U73122 or (-)-xestospongin C (Xesto) for 30 to 60 min at 37°C. The cells were washed and loaded with Fura-2AM before being exposed to EHV-4gH1. Release of $Ca^{2+}$ was monitored, and images were captured at the indicated time points. Viruses were added at the 50-s time point. (B) Fluorescence intensity of Fura-2AM as a function of time after exposure of ED cells to EHV-4gH1 in the presence or absence of U73122 or (−)-xestospongin C. The data show averages from 3 independent experiments. $P < 0.001$ indicates a significant difference between EHV-4gH1 in the presence and absence of the used inhibitors.

**TABLE 1** List of all inhibitors used in the study

| Inhibitor | Concn | Function |
|---|---|---|
| Genistein | 100 $\mu$g/ml | Tyrosine kinase inhibitor |
| Dynasore | 80 $\mu$M | Dynamin-II inhibitor |
| 2-APB | 100 $\mu$M | $IP_3R$ inhibitor |
| Verapamil | 10 $\mu$M | $Ca^{2+}$ channel blocker |
| BAPTA-AM | 50 $\mu$M | Cell-permeable cytosolic $Ca^{2+}$ chelator |
| (−)-Xestospongin C | 1 $\mu$M | Potent and specific inhibitor of $IP_3R$ |
| U73122 | 10 $\mu$M | Potent and specific inhibitor of PLC |
| Thapsigargin | 10 $\mu$M | Inhibitor of sarco-endoplasmic reticulum $Ca^{2+}$ ATPases |
| Ionomycin | 2 $\mu$M | Ionophore that raises intracellular calcium level |
| Latrunculin B | 10 nM | Induces actin cytoskeleton depolymerization |
| R5421 | 1–100 $\mu$M | Scramblase inhibitor, ethanimidothioic acid *N*-[(*N*-butylthio-*N*-methylamino)-carbonyloxy]-methyl ester |

nism. As a control of actin depolymerization, cells were treated with latrunculin B for 15 min (51), which resulted in a reduction of F-actin in ED cells as expected (see Fig. S5A).

## DISCUSSION

Viruses have to overcome a number of barriers in order to be able to deliver their genomes into cells and then spread from cell to cell. Routing the entry pathway through manipulation of cell signaling cascades is one of the strategies used by HSV-1 (18) as well as EHV-1 (22). EHV-1 can enter ED cells through a mechanism that requires gD–MHC-I receptor interaction and gH–$\alpha_4\beta_1$-integrin interaction, which ultimately results in gB-mediated fusion of the viral envelope with the plasma membrane (5, 22). Disruption of the gH-integrin interaction redirects the virus to a caveolin/raft-dependent endocytic pathway and also results in productive infection (22). In the present study, we show that EHV-1 binding to its receptors on the plasma membrane induces release of $Ca^{2+}$ from intracellular stores in equine epithelial cells. Our results suggest that the release of $Ca^{2+}$ is initiated by the interaction between gH and $\alpha_4\beta_1$-integrin with subsequent activation of PLC and generation of $IP_3$ that binds to $IP_3R$ and mobilizes $Ca^{2+}$ from ER stores. $Ca^{2+}$ release also activated phospholipid scramblase, which resulted in exposure of PS on the plasma membrane. Blocking of increased cytosolic $Ca^{2+}$ levels as well as inhibition of PS exposure redirected many EHV-1 particles to a caveolin-dependent endocytic pathway, indicating that virus fusion at the plasma membrane may be enhanced in response to $Ca^{2+}$ and subsequent exposure of PS (Fig. 10).

We proposed earlier that the gH–$\alpha_4\beta_1$-integrin interaction likely activates specific signals that regulate virus entry (22). Consistent with our hypothesis, we were able to show here that an increase in cytosolic $Ca^{2+}$ was triggered only in the presence of gH1 (EHV-1 and EHV-4gH1) shortly after adding the viruses to the cells. In contrast, EHV-1gH4, EHV-1gH$^{S440A}$, and EHV-4 were not able to induce a significant increase in cytosolic $Ca^{2+}$—we surmise as a consequence of the failure of gH4 to interact with integrins. Similarly, blocking the interaction of gH1 and integrins, by means of either using $\alpha_4\beta_1$-integrin blocking antibodies or soluble $\alpha_4\beta_1$-integrins, also inhibited the increase in cytosolic $Ca^{2+}$. It is worth mentioning that only $\alpha_4\beta_1$-integrin blocking antibodies, but not other integrin antibodies, such as anti-$\alpha_4\beta_7$ or anti-$\alpha_V\beta_5$, could affect the entry pathway of EHV-1 (22). Furthermore, heat-inactivated viruses that still can bind to the cells were also able to induce $Ca^{2+}$ release. Our results suggest that virus binding to cell surface integrins is sufficient to trigger cytosolic $Ca^{2+}$ increase. Our results are consistent with a previous study, which showed that activation of a 92.5-kDa cellular receptor by the HCMV gH-gL complex can activate signaling cascades responsible for elevation of cytosolic $Ca^{2+}$ concentrations (52). In the case of HSV-1, it was postulated that the complete set of the essential glycoproteins utilized for virus entry (gB, gD, and gH-gL) is required to trigger calcium release (37). Furthermore, it has been shown that binding of HSV-1- and HSV-2-gH to surface $\alpha_v$-integrins triggers the release of $IP_3R$-dependent intracellular $Ca^{2+}$ stores (53, 54). These results together with our observation may point to a common pathway for herpesvirus entry that is initiated by interactions of gH with integrins that ultimately signal intracellularly to ensure efficient nucleocapsid translocation into the cytoplasm.

Similar to other viruses (e.g., HIV-1 [55], hepatitis C virus [56], rotavirus [57], coxsackievirus [CVB] [58], and HSV [37]), EHV-1 mediates, upon receptor binding, an increase in cytosolic $Ca^{2+}$ by the activation of the PLC-$IP_3R$-signaling pathway. Pretreatment of the cells with either U73122 or (-)-xestospongin C, two potent and specific inhibitors of PLC and $IP_3R$, respectively (59–61), inhibited the flux of $Ca^{2+}$ into the cytosol. However, we could not test the effect of small interfering RNA (siRNA) to specifically knock down PLC or $IP_3R$ due to the very low transfection efficiency that can be achieved in primary ED cells. We propose that after virion attachment to cells through gC (62), engagement of the receptor and irreversible binding through gD (5, 63), as well as interaction of gH with $\alpha_4\beta_1$-integrins (22), a signal cascade is induced involving PLC activation, which then triggers $IP_3$-mediated $Ca^{2+}$ release from the ER.

To assess the role of cytosolic $Ca^{2+}$ in deciding the entry pathway of EHV-1, cells were pretreated with a number of inhibitors that can block $Ca^{2+}$ release from ER or influx through different mechanisms. The data show that these inhibitors alone did not affect the rate of virus infection. Furthermore, interrupting the endocytic pathway with either dynasore, DynII-K44A, or genistein alone had no effect on EHV-1 infection rates. However, double inhibition with dynasore or genistein or simultaneous treatment of DynII-K44A-transfected cells with one of the calcium inhibitors significantly reduced virus infection. In addition, we could detect significant colocalization of virus particles with Cav-1, but not clathrin, only after blocking cytosolic $Ca^{2+}$ increase.

We surmised that the activation of $Ca^{2+}$-signaling pathways may trigger membrane fusion of EHV-1 to proceed, but the question remained as to how that can be achieved. Based on the im-

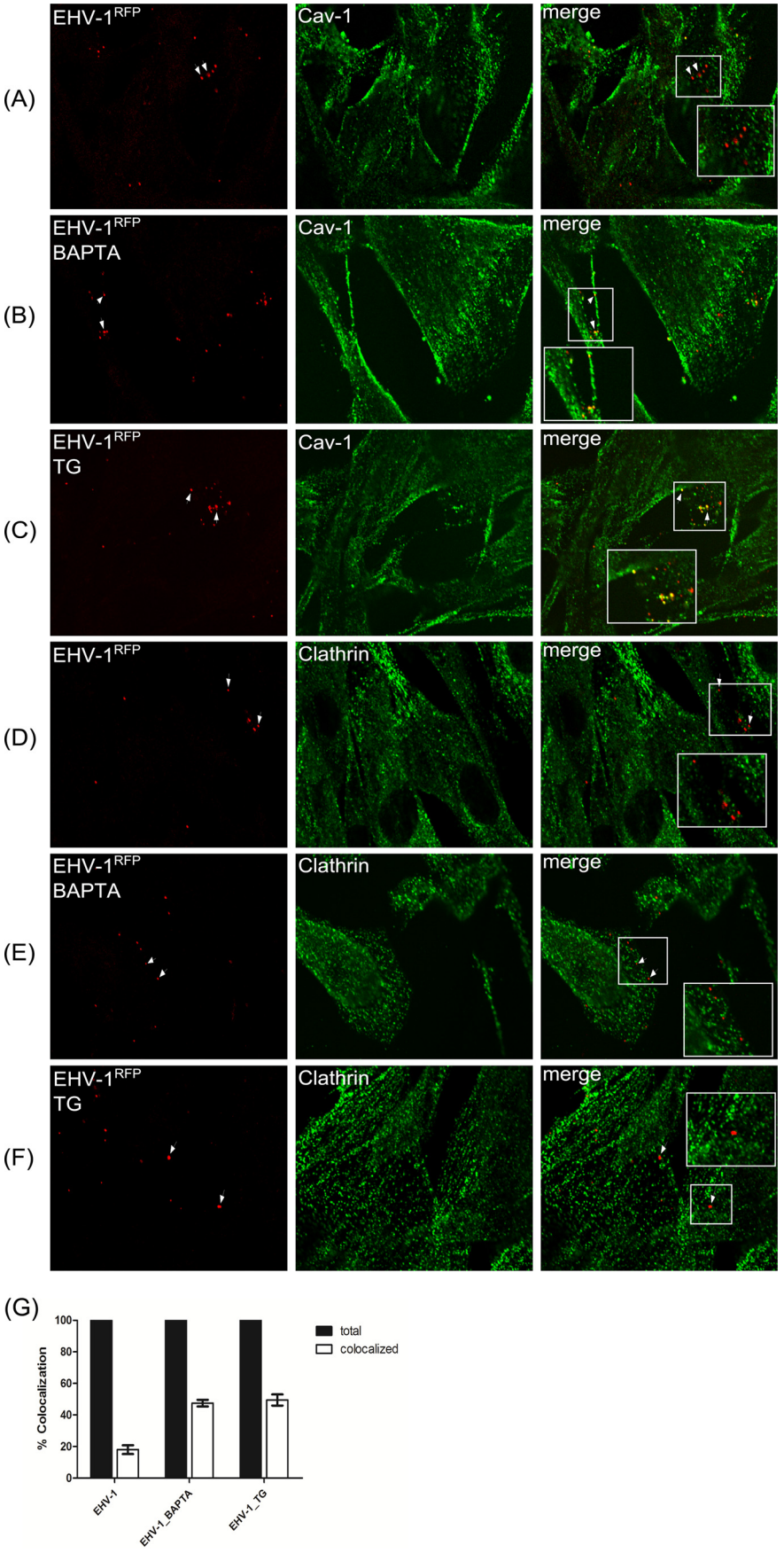
(A)
EHV-1RFP
Cav-1
merge
(B)
EHV-1RFP
BAPTA
Cav-1
merge
(C)
EHV-1RFP
TG
Cav-1
merge
(D)
EHV-1RFP
Clathrin
merge
(E)
EHV-1RFP
BAPTA
Clathrin
merge
(F)
EHV-1RFP
TG
Clathrin
merge
(G)
% Colocalization
100
80
60
40
20
0
EHV-1
EHV-1_BAPTA
EHV-1_TG
total
colocalized

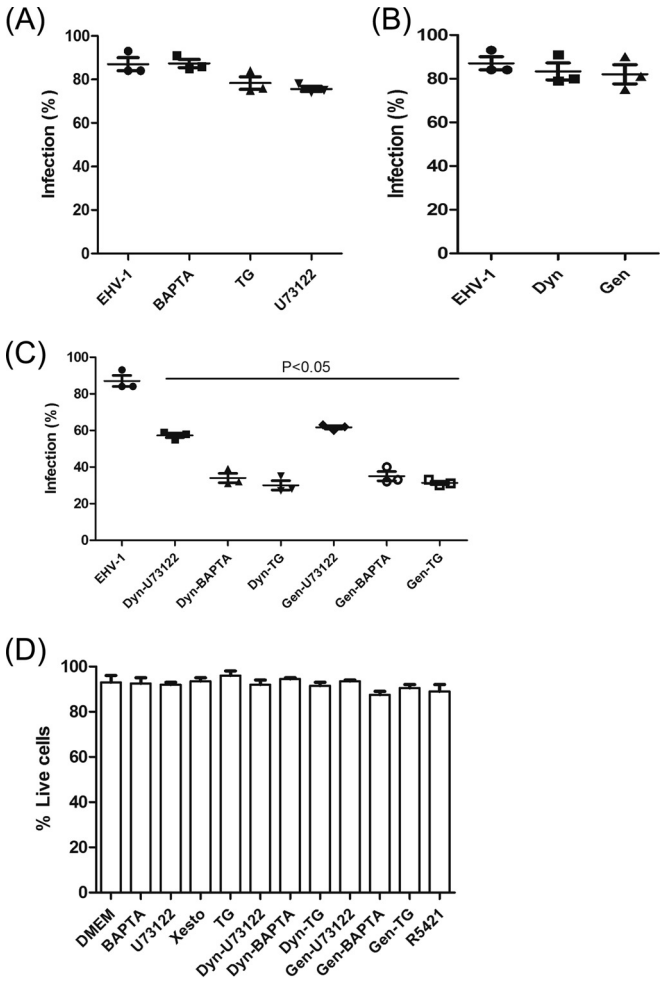


**FIG 7** Effect of different inhibitors on EHV-1 infection. For treatment with a single inhibitor, ED cells were treated with BAPTA-AM, thapsigargin (TG), or U73122 (A) or dynasore (Dyn), or genistein (Gen) (B). (C) In the case of two inhibitors, the different inhibitor combinations are indicated. The cells were then infected with EHV-1 (MOI of 5) for 8 to 12 h. The percentage of infected cells was determined by flow cytometry. Error bars represent the means ± standard deviations from 3 independent experiments. $P < 0.05$ indicates a significant difference for means compared to the parental virus without inhibitor treatment. (D) Toxicity assays of pharmacological inhibitors on ED cells. Propidium iodide (PI) uptake is shown in cells following incubation for 8 to 12 h with the indicated inhibitors. The number of live cells (no PI uptake) relative to total cell numbers was determined after flow cytometric analysis and is given as a percentage. Error bars represent the means ± standard deviations from 2 independent experiments.

portance of lipid mixing in virus-cell fusion events (64) and the fact that $Ca^{2+}$ is known to change the lipid arrangement in membranes, we examined the level of PS exposure on the outer leaflet in response to the dramatic cytosolic $Ca^{2+}$ increase after virus binding. Anionic lipids such as bis(monoacylglycero)phosphate and PS are mainly located in the inner leaflet of the plasma membrane (65). Rapid collapse of lipid asymmetry is mediated by ATP-independent and $Ca^{2+}$-dependent phospholipid scramblases, which cause lipid scrambling between the inner and outer leaflet, ultimately leading to the exposure of PS on the plasma membrane (66). PS has been shown to enhance virus fusion with endosomal membranes, where the virus encounters anionic lipids for the first time during entry (67, 68). In addition, the E1 protein of rubella virus specifies a unique metal-binding site, which is reminiscent of the metal-ion-dependent ligand-binding site of the T-cell immunoglobulin and mucin (TIM) family proteins that specifically bind PS on membranes (69). It was shown that $Ca^{2+}$ is strictly required for E1-membrane fusion and virus infection (70). Consistent with these effects observed in other enveloped viruses, we show here that, upon binding, EHV-1 induces PS exposure on the cell surface through a $Ca^{2+}$- and scramblase-dependent mechanism. Treatment of cells with an inhibitor of $Ca^{2+}$ release from the ER or a scramblase inhibitor blocked PS exposure induced by EHV-1. Of note, EHV-1 entry receptor (MHC-I) levels or distribution was not affected by the increased exposure of PS, indicating that PS may play a role in influencing virus entry by facilitating lipid mixing. Additionally, we found that most of the virus particles colocalized with PS; however, it is not clear how any of the viral glycoproteins (particularly, the fusogenic protein gB) interact with PS (69, 71). Apart from direct interaction of PS with viral glycoproteins, the elevated level of PS on the plasma membrane may influence virus entry through differential packing of lipids, modifying membrane fluidity, or promoting local changes in the bilayer phase (64). However, the exact mechanism will require detailed biophysical studies. Besides PS exposure on the cell surface, $Ca^{2+}$ may contribute to maintaining sufficient levels of ATP and other metabolites that protect cells from damage or could allow high-affinity binding of glycoproteins to cell surface receptors (72, 73). We currently exclude that reorganization of the actin cytoskeleton through intracellular signaling facilitates virus internalization (49, 50), as we were unable to find actin rearrangements after EHV-1 binding and infection.

In our previous work, we proposed a model based on the finding that fusion of the viral envelope with the plasma membrane can only occur if a strong interaction between EHV-1 gH and $\alpha_4\beta_1$-integrins was established. Once this interaction is disrupted, fusion with the plasma membrane cannot occur any longer, and the virus is redirected to the endocytic pathway in order to establish an infection. Here, we further show that gH-integrin interaction resulted in a dramatic increase in cytosolic $Ca^{2+}$, which resulted in PS scrambling. We hypothesize that this virus-induced change in lipid composition apparently facilitates virus entry (Fig. 10).

The fact that EHV-4 harboring gH1, in contrast to EHV-4, was able to induce $Ca^{2+}$ signaling supports our hypothesis that gH–$\alpha_4\beta_1$-integrin interaction is essential for $Ca^{2+}$ release. Further studies will be needed to address the role of $Ca^{2+}$ during the entry of EHV-4gH1. We consider our findings important for understanding herpesvirus (particularly EHV-1) entry, and our results may allow the design of effective therapeutics that can be implemented for prevention of infection and disease.

**FIG 6** Colocalization of viral particles with caveolin. ED cells were incubated with EHV-$1^{RFP}$ (MOI of 20) at 4°C for 2 h. Cells were incubated with either BAPTA-AM (B and E) or thapsigargin (TG [C and F]) before infection. The medium was replaced with preheated medium at 37°C, and cells were fixed at 5 min after shifting the temperature. Cells were stained with anti-Cav-1 (green [A to C]) or anti-clathrin (green [D to F]). (G) The percentages of virus particles colocalizing with caveolin after infection with EHV-$1^{RFP}$ and in the presence of inhibitors were determined in randomly selected fields of infected ED cells.

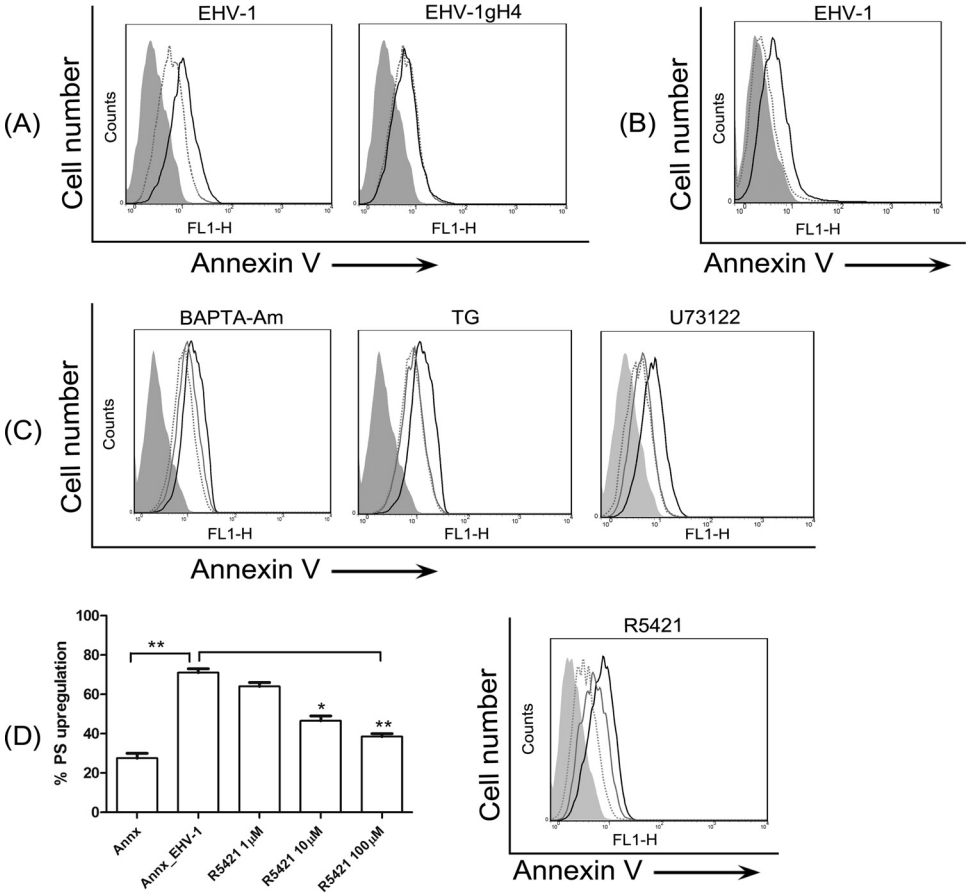


**FIG 8** EHV-1 binding induces PS scrambling. (A) ED cells were incubated with EHV-1 or EHV-1gH4 and stained with FITC-labeled annexin V for detection of surface PS levels. Dotted lines, mock-infected cells stained with annexin V; solid black lines, virus-infected cells stained with annexin V. (B) Cells were incubated with EHV-1 and stained with FITC-labeled annexin V at 4°C. Dotted lines, mock-infected cells; solid black lines, EHV-1-infected cells. (C) Cells were treated with BAPTA-AM, thapsigargin (TG), or U73122 before infection with EHV-1. Cells were stained with FITC-labeled annexin V. Dotted lines, mock-infected cells; solid black lines, EHV-1-infected cells; gray lines, EHV-1-infected cells treated with different inhibitors. (D) Dose-dependent effect of the scramblase inhibitor. Cells were either mock infected or infected with EHV-1 in the presence of increasing concentrations of R5421 (left panel [*, $P < 0.05$; **, $P < 0.001$]) or with 100 $\mu$M R5421 (right panel). Surface-exposed PS was detected with FITC-labeled annexin V. Dotted line, mock-infected cells; solid black line, EHV-1-infected cells; gray line, EHV-1-infected cells treated with R5421. Data are from one representative experiment out of three.

## MATERIALS AND METHODS

**Cells and viruses.** Equine dermal (ED) cells (Friedrich-Loeffler Institute, Greifswald-Insel Riems, Germany) were propagated in Iscove's modified Dulbecco's medium (IMDM [Invitrogen]) supplemented with 20% fetal bovine serum (FBS [Biochrom]). The parental EHV-1 strain L11Δgp2 (74), the parental EHV-4 strain WA79 recovered from an infectious bacterial artificial chromosome (BAC) clone (75), the EHV-1 mutant harboring gH4 (EHV-1gH4), EHV-4gH1, and EHV-1gH$^{S440A}$ (39), as well as EHV-1 with monomeric red fluorescent protein (mRFP)-labeled nucleocapsids (EHV-1$^{RFP}$) (22) were grown on ED cells supplemented with $Ca^{2+}$-free minimal essential medium (MEM). Heat-inactivated (HI) virus was prepared by heating the virus to 56°C for 1 h, as described before (37, 40). All infected cultures were freeze-thawed twice and centrifuged to remove cellular debris, and their titer was determined by plaque assay on ED cells as described before (63). All recombinant viruses express the enhanced green fluorescent protein (eGFP) marker for rapid detection of infected cells.

**Inhibitors.** Genistein (100 $\mu$g/ml), dynasore (80 $\mu$M), and 2-APB (100 $\mu$M) were purchased from Sigma and diluted in dimethyl sulfoxide (DMSO) to the given concentrations (Table 1). Verapamil (10 $\mu$M) and the cell-permeable cytosolic $Ca^{2+}$ chelator BAPTA-AM (50 $\mu$M) were obtained from Calbiochem and diluted in DMSO. (−)-Xestospongin C (1 $\mu$M), the PLC inhibitor U73122 (10 $\mu$M), thapsigargin (10 $\mu$M), and ionomycin (2 $\mu$M) were purchased from Tocris Biosciences (diluted in DMSO). Latrunculin B was obtained from Cayman Chemical and diluted in ethanol. The scramblase inhibitor R5421, ethanimidothioic acid *N*-[(*N*-butylthio-*N*-methylamino)-carbonyloxy]-methyl ester (100 $\mu$M), was obtained from Endotherm and dissolved in DMSO (45). The final concentration of DMSO added to the cells was equal to or less than 0.01% of the total volume of the medium in all cases. Toxicity assays were performed to ensure that inhibitors did not have toxic effect when used with the cells (Fig. 7D).

**Cytosolic $Ca^{2+}$ imaging.** Cells were grown on glass bottom 35-mm-diameter MatTek dishes (MatTek Corporation), loaded with 1 $\mu$M Fura-2AM (Enzo Life Sciences) prepared in $Ca^{2+}$-free MEM for 30 min at 37°C, and rinsed 3 times with $Ca^{2+}$- and $Mg^{2+}$-free phosphate-buffered saline (PBS). The cells were either exposed directly to the viruses (parental, HI, or mutant virus at a multiplicity of infection [MOI] of 1), incubated with $Ca^{2+}$-free medium, which was obtained from the supernatant of noninfected cultures after freezing and thawing and used as a negative control, or pretreated with the drugs for 30 to 60 min before being exposed to the viruses. For blocking of integrins, cells were incubated with 20 $\mu$g/ml of MAb P4C2, an $\alpha_4\beta_1$-integrin antagonist (Abcam), for 60 min at 37°C. In some experiments, the viruses were pretreated with soluble $\alpha_4\beta_1$-integrin

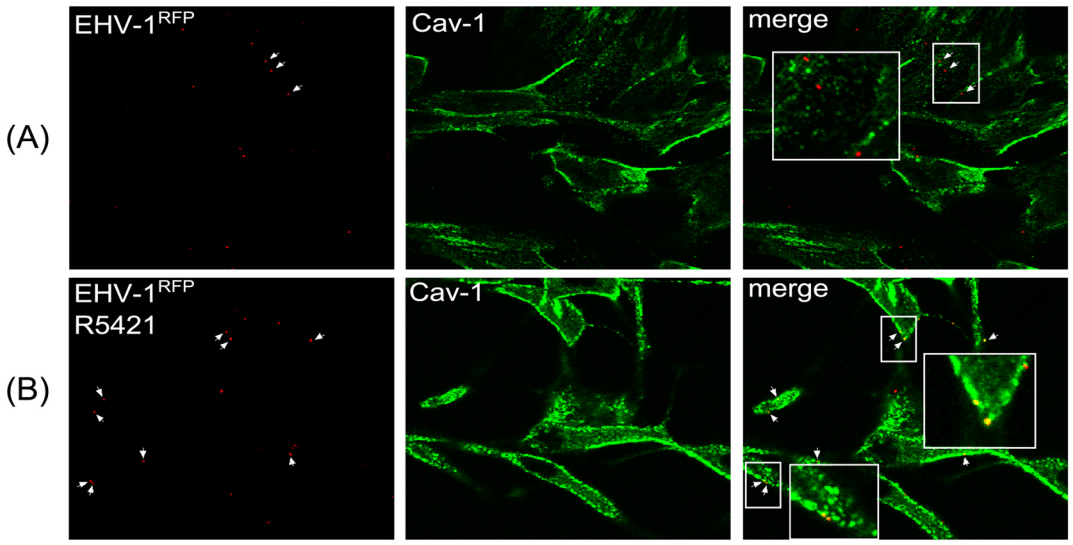
(A)
EHV-1RFP
Cav-1
merge
(B)
EHV-1RFP
R5421
Cav-1
merge

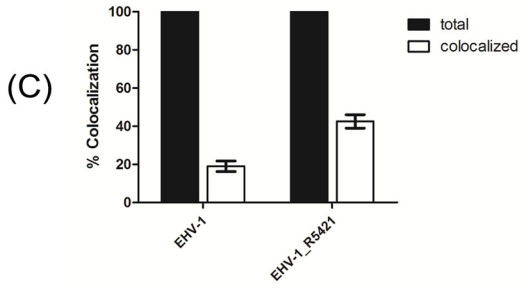
(C)
% Colocalization
100
80
60
40
20
0
EHV-1
EHV-1_R5421
total
colocalized

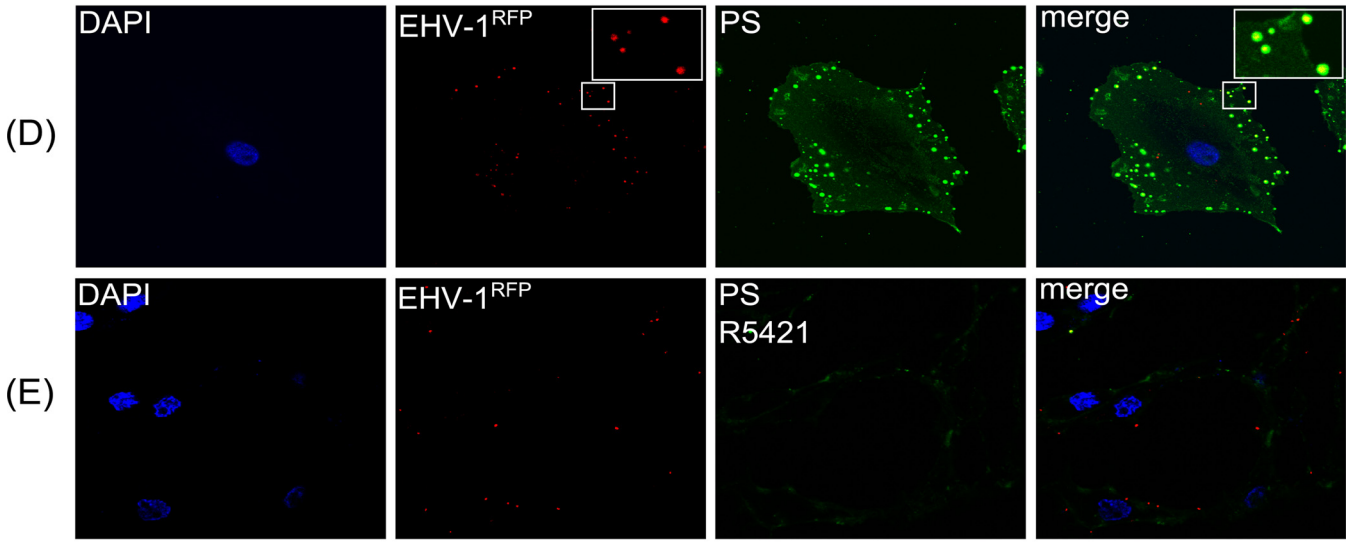
(D)
DAPI
EHV-1RFP
PS
merge
(E)
DAPI
EHV-1RFP
PS
R5421
merge

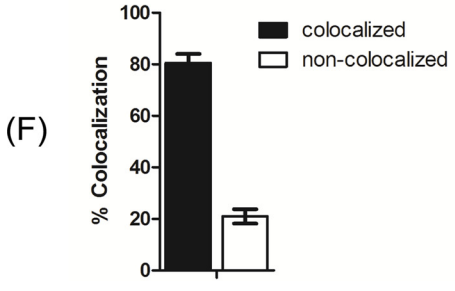
(F)
% Colocalization
100
80
60
40
20
0
colocalized
non-colocalized

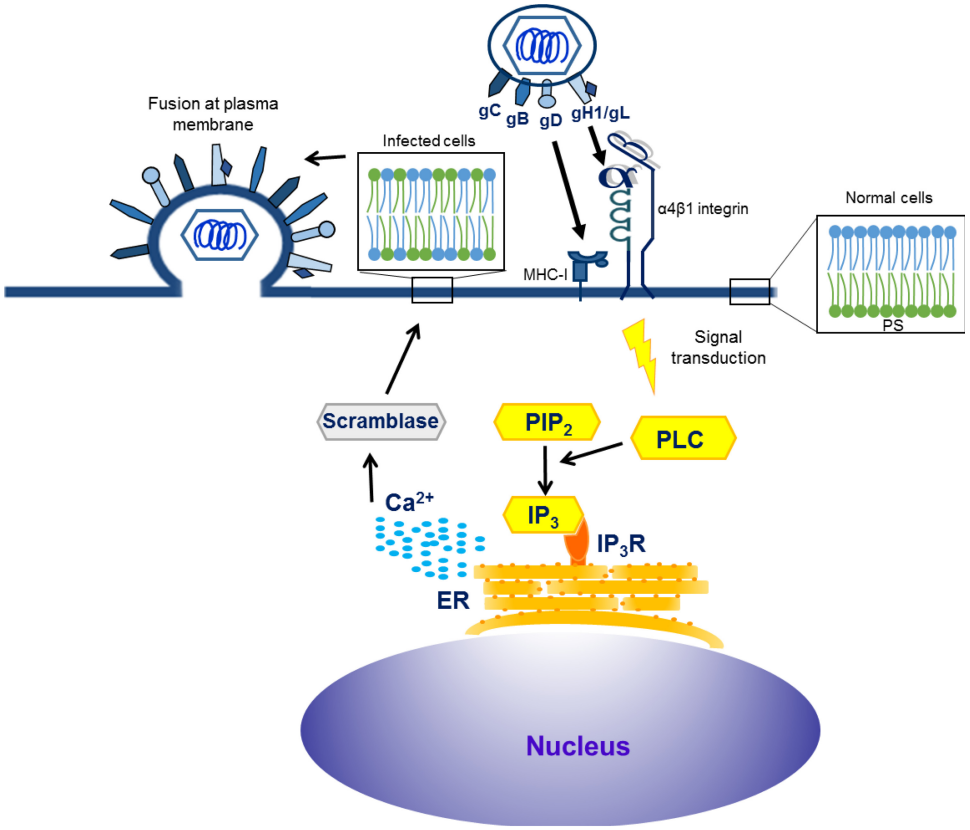


**FIG 10** Proposed model of EHV-1 entry into equine epithelial cells. Virions initially bind to target (ED) cells through gD–MHC-I interaction, followed by activation of the gH/gL complex that interacts with $\alpha_4\beta_1$-integrin. Interaction of gH with $\alpha_4\beta_1$-integrin results in the activation of PLC and generation of $IP_3$ that binds to $IP_3R$ and mobilizes $Ca^{2+}$ from the ER. The release of $Ca^{2+}$ activates scramblase, which exposes PS on cell surface. Scrambling of PS may facilitate fusion of EHV-1 at the plasma membrane. Blocking the gH-integrin interaction inhibits PS exposure and reroutes the virus to the endocytic pathway.

(15 $\mu$g/ml; R&D Systems) (22) for 60 min at 37°C before addition to cells. Images were captured with an inverted fully motorized epifluorescence microscope (Olympus X-81) equipped with a highly sensitive cooled charge-coupled device (CCD) RT slider camera (Diagnostic Instruments). Cells were visualized with a 60×/1.35 oil objective (Zeiss), and images were acquired using MetaView imaging acquisition and analysis software (Molecular Devices). Fura-2AM-loaded cells were excited at 340 and 380 nm, and images were captured every 5 s for 10 min in three independent experiments. Fluorescence intensities for excited cells (10 to 12 individual cells) were calculated using MetaView, and replicates were averaged and plotted as a function of time. Images were colored with the MetaView imaging software in order to better visualize cytosolic $Ca^{2+}$ increase. Yellow indicates low cytosolic $Ca^{2+}$, while red indicates high cytosolic $Ca^{2+}$.

**Effect of inhibitors on the virus entry pathway.** ED cells were pretreated with different inhibitors for 30 to 60 min, depending on the drug, at 37°C before infection with the viruses (MOI of 5) in the presence of the drugs. After 8 to 12 h, cells were trypsinized and washed twice with PBS. After centrifugation, cells were suspended in PBS, and 10,000 cells were analyzed with a FACSCalibur flow cytometer (BD Biosciences) to determine the percentage of infected cells by fluorescence emission. For the PLC inhibitor U73122, cells were treated with the inhibitor for 30 min. Before infection, the inhibitor was removed, and the cells were washed with PBS to avoid any toxic effect on the cells.

ED cells were transfected with wt-DynII or DynII-K44A plasmids using Nucleofector (Lonza) (76), and the efficiency of transfection was determined by Western blot analysis. Transfected cells were then infected with EHV-1 in the presence or absence of different inhibitors for 12 h before the samples were collected for plaque assay (77).

**Binding assay.** ED cells were incubated with either EHV-1 or EHV-1-HI viruses for 2 h at 4°C. Cells were then washed with ice-cold PBS, incubated with EHV-1 anti-gB MAb at 4°C for 1 h, stained with Alexa Fluor 488-labeled goat anti-mouse IgG at 4°C, and analyzed by flow cytometry (63). As a control, cells were also stained with the primary and secondary antibodies without prior virus binding. In another experiment, ED cells were infected with either EHV-1 or EHV-1-HI viruses for 24 h at 37°C. The percentage of infected cells was detected by flow cytometry.

**Internalization assay using confocal microscopy.** ED cells were seeded into 35-mm gridded MatTek dishes. EHV-$1^{RFP}$ (20 PFU/cell) was allowed to attach to the cells for 2 h at 4°C. After removal of unabsorbed viruses by thorough washing (three consecutive washes), prewarmed medium was added, and the cells were shifted to 37°C for 5 min. In another experiment, cells were first incubated with BAPTA-AM (50 $\mu$M), thapsigargin (10 $\mu$M), or R5421 (100 $\mu$M) for 1 h before infection with EHV-

**FIG 9** Colocalization of EHV-1-labeled particles with caveolin after scramblase inhibition. (A and B) ED cells were incubated with EHV-$1^{RFP}$ (MOI of 20) at 4°C for 2 h in the absence (A) or presence (B) of R5421, and cells were stained with anti-Cav-1 antibody. (C) The percentage of EHV-1-labeled particles colocalizing with caveolin in the presence of R5421 was determined in randomly selected fields of infected ED cells. (D and E) Colocalization of EHV-1 with PS. ED cells were incubated with EHV-$1^{RFP}$ in the absence (D) or presence (E) of R5421. Surface PS was stained with FITC-labeled annexin V. (F) The percentage of EHV-1-labeled particles colocalizing with PS was determined in randomly selected fields of infected ED cells.

$1^{RFP}$. Cells were fixed with 4% paraformaldehyde and permeabilized with 0.1% saponin. Caveolin-1 or clathrin was detected with polyclonal antibodies directed against Cav-1 or the clathrin heavy chain, respectively (Abcam). The specificity of the anti-Cav-1 and anti-clathrin-heavy-chain antibodies in ED cells had been examined by Western blotting and indirect immunofluorescence assays (22). For fluorescence microscopy, cells were inspected with an Olympus Fluoview FV-1000MPE confocal laser scanning microscope using a 60×/1.35 oil immersion objective.

**PS exposure on cell surface.** ED cells were trypsinized, washed with $Ca^{2+}$- and $Mg^{2+}$-free PBS, and resuspended in $Ca^{2+}$-free MEM. EHV-1 or EHV-1gH4 (MOI of 1) was allowed to attach to the cells for 1 h at 4°C. Mock-infected cells were used as a control. After removal of unbound viruses, ice-cold or prewarmed medium was added, and the cells were further incubated on ice or shifted to 37°C for 5 min, respectively. In another experiment, cells were first incubated with BAPTA-AM (50 $\mu$M), thapsigargin (10 $\mu$M), U73122 (10 $\mu$M), or R5421 (1 to 100 $\mu$M) for 1 h before infection with EHV-1. Cells were then stained with fluorescein isothiocyanate (FITC)-labeled annexin V (BD Biosciences) at 4 or 37°C according to the manufacturer's instructions. Following washing with annexin V-binding buffer and PBS, cells were resuspended in PBS supplemented with propidium iodide (PI [Molecular Probes]) at a final concentration of 10 $\mu$g/ml, and 10,000 PI-negative cells were analyzed to determine the percentage of PS expression using flow cytometry. Flow cytometry data were analyzed using FlowJo software (Treestar).

For confocal microscopy, ED cells were seeded on glass coverslips placed in 24-well plates. EHV-$1^{RFP}$ (20 PFU/cell) was allowed to attach to the cells for 1 h at 4°C in the presence or absence of R5421 (100 $\mu$M). Unbound viruses were removed by washing, prewarmed medium was added, and the cells were shifted to 37°C for 5 min. Mock-infected or staurosporine-treated (1 $\mu$M [Sigma]) cells were used as controls. Cells were fixed with 4% paraformaldehyde and stained with FITC-labeled annexin V. Coverslips were mounted onto glass slides using Vectashield-with 4′,6-diamidino-2-phenylindole (DAPI) (Vector Laboratories), and cells were inspected with an Olympus Fluoview FV-1000MPE confocal laser scanning microscope using a 60×/1.35 oil immersion objective.

**MHC-I expression on cell surface.** ED cells were grown on glass coverslips in a 24-well plate and either infected with viruses (MOI of 1), as indicated in Fig. S3, or supplemented with 20 mM $CaCl_2$. After 1-h incubation at 4°C, prewarmed medium was added and the cells were shifted to 37°C for 5 min. To evaluate the level of MHC-I expression, cells were trypsinized and incubated with the anti-equine MHC-I monoclonal antibody (MAb) CZ3 (27) for 1 h at room temperature. After two washes with PBS, cells were incubated with Alexa Fluor 488-labeled goat anti-mouse IgG (Invitrogen [1:500 dilution]), and 10,000 cells were analyzed with a FACSCalibur flow cytometer. The intensity of fluorescence was analyzed using FlowJo software.

To evaluate MHC-I distribution on cell surface, infected or calcium-supplemented cells were fixed with 4% paraformaldehyde and blocked with 2% bovine serum albumin (BSA [Applichem]). Surface MHC-I was stained with anti-MHC-I CZ3 MAb and finally with Alexa Fluor 488-labeled goat anti-mouse IgG. After being washed three times, coverslips were mounted onto glass slides using Vectashield-with DAPI. The cells were imaged by immunofluorescence microscopy (Zeiss Axio imager M1), and pictures were taken with an AxioCam CCD camera (Zeiss).

**Labeling and quantification of actin filaments.** ED cells were grown on glass coverslips and infected with EHV-1, EHV-1gH4, EHV-4, or EHV-4gH1. Infected cells were fixed with 4% paraformaldehyde and permeabilized with 0.1% saponin. After undergoing blocking with 2% bovine serum albumin (BSA), F-actin was labeled with phalloidin-Alexa Fluor 568 (1:40; Invitrogen) for 15 min. Virus-infected cells were stained with anti-gB antibodies and labeled with Alexa Fluor 488. After being washed three times, coverslips were mounted onto glass slides using Vectashield-with DAPI, the cells were imaged by immunofluorescence microscopy (Zeiss Axio imager M1), and pictures were taken with an AxioCam CCD camera (Zeiss).

For quantification of F-actin (51), ED cells were either treated with latrunculin B (10 nM) for 15 min or infected with different viruses for either 5 or 60 min after incubation, and then the cells were fixed, permeabilized, and stained with phalloidin-Alexa Fluor 647 (1:1,000; Santa Cruz Biotechnology). Cells were analyzed on FACSCalibur.

**Statistical analysis.** Using Prism software (GraphPad), one-way analysis of variance (ANOVA) and Student's *t* test were used to test for significance. The data are given as means, and error bars show standard deviations.

## SUPPLEMENTAL MATERIAL

Supplemental material for this article may be found at http://mbio.asm.org/lookup/suppl/doi:10.1128/mBio.01552-15/-/DCSupplemental.

Movie S1, AVI file, 4.3 MB.
Movie S2, AVI file, 3 MB.
Movie S3, MP4 file, 3 MB.
Movie S4, AVI file, 3.8 MB.
Figure S1, EPS file, 0.1 MB.
Figure S2, EPS file, 0.2 MB.
Figure S3, TIF file, 2.6 MB.
Figure S4, TIF file, 2 MB.
Figure S5, TIF file, 2.5 MB.

## ACKNOWLEDGMENTS

We thank Maik J. Lehmann and Thomas Korte, Humboldt-Universität zu Berlin, Germany, for sharing their confocal microscopy expertise. We thank Michaela Zeitlow, Freie Universität Berlin, Germany, for technical assistance.

This study was supported by a grant from the DFG to W.A. (AZ 97/3-1) and to A.H. (HE 3763/15).

## REFERENCES

1. **Campadelli-Fiume G, Menotti L, Avitabile E, Gianni T.** 2012. Viral and cellular contributions to herpes simplex virus entry into the cell. Curr Opin Virol **2:**28–36. http://dx.doi.org/10.1016/j.coviro.2011.12.001.
2. **Gianni T, Cerretani A, Dubois R, Salvioli S, Blystone SS, Rey F, Campadelli-Fiume G.** 2010. Herpes simplex virus glycoproteins H/L bind to cells independently of $\alpha V\beta 3$ integrin and inhibit virus entry, and their constitutive expression restricts infection. J Virol **84:**4013–4025.
3. **Sasaki M, Hasebe R, Makino Y, Suzuki T, Fukushi H, Okamoto M, Matsuda K, Taniyama H, Sawa H, Kimura T.** 2011. Equine major histocompatibility complex class I molecules act as entry receptors that bind to equine herpesvirus-1 glycoprotein D. Genes Cells **16:**343–357. http://dx.doi.org/10.1111/j.1365-2443.2011.01491.x.
4. **Spear PG.** 2004. Herpes simplex virus: receptors and ligands for cell entry. Cell Microbiol **6:**401–410. http://dx.doi.org/10.1111/j.1462-5822.2004.00389.x.
5. **Azab W, Harman R, Miller D, Tallmadge R, Frampton AR, Jr, Antczak DF, Osterrieder N.** 2014. Equine herpesvirus type 4 (EHV-4) uses a restricted set of equine major histocompatibility complex class I proteins as entry receptors. J Gen Virol **95:**1554–1563. http://dx.doi.org/10.1099/vir.0.066407-0.
6. **Fuller AO, Spear PG.** 1987. Anti-glycoprotein D antibodies that permit adsorption but block infection by herpes simplex virus 1 prevent virion-cell fusion at the cell surface. Proc Natl Acad Sci U S A **84:**5454–5458. http://dx.doi.org/10.1073/pnas.84.15.5454.
7. **Nicola AV, Hou J, Major EO, Straus SE.** 2005. Herpes simplex virus type 1 enters human epidermal keratinocytes, but not neurons, via a pH-dependent endocytic pathway. J Virol **79:**7609–7616. http://dx.doi.org/10.1128/JVI.79.12.7609-7616.2005.
8. **Richart SM, Simpson SA, Krummenacher C, Whitbeck JC, Pizer LI, Cohen GH, Eisenberg RJ, Wilcox CL.** 2003. Entry of herpes simplex virus type 1 into primary sensory neurons in vitro is mediated by nectin-1/HveC. J Virol **77:**3307–3311. http://dx.doi.org/10.1128/JVI.77.5.3307-3311.2003.
9. **Wittels M, Spear PG.** 1991. Penetration of cells by herpes simplex virus does not require a low pH-dependent endocytic pathway. Virus Res **18:**271–290. http://dx.doi.org/10.1016/0168-1702(91)90024-P.
10. **Fan Q, Amen M, Harden M, Severini A, Griffiths A, Longnecker R.**

2012. Herpes B virus utilizes human nectin-1 but not HVEM or PILRalpha for cell-cell fusion and virus entry. J Virol **86:**-4468–4476. http://dx.doi.org/10.1128/JVI.00041-12.
11. **Gianni T, Campadelli-Fiume G, Menotti L.** 2004. Entry of herpes simplex virus mediated by chimeric forms of nectin1 retargeted to endosomes or to lipid rafts occurs through acidic endosomes. J Virol **78:**12268–12276. http://dx.doi.org/10.1128/JVI.78.22.12268-12276.2004.
12. **Mercer J, Schelhaas M, Helenius A.** 2010. Virus entry by endocytosis. Annu Rev Biochem **79:**803–833. http://dx.doi.org/10.1146/annurev-biochem-060208-104626.
13. **Milne RSB, Nicola AV, Whitbeck JC, Eisenberg RJ, Cohen GH.** 2005. Glycoprotein D receptor-dependent, low-pH-independent endocytic entry of herpes simplex virus type 1. J Virol **79:**6655–6663. http://dx.doi.org/10.1128/JVI.79.11.6655-6663.2005.
14. **Nicola AV, McEvoy AM, Straus SE.** 2003. Roles for endocytosis and low pH in herpes simplex virus entry into HeLa and Chinese hamster ovary cells. J Virol **77:**5324–5332. http://dx.doi.org/10.1128/JVI.77.9.5324-5332.2003.
15. **Nicola AV, Straus SE.** 2004. Cellular and viral requirements for rapid endocytic entry of herpes simplex virus. J Virol **78:**7508–7517. http://dx.doi.org/10.1128/JVI.78.14.7508-7517.2004.
16. **Rahn E, Petermann P, Hsu M, Rixon FJ, Knebel-Mörsdorf D.** 2011. Entry pathways of herpes simplex virus type 1 into human keratinocytes are dynamin- and cholesterol-dependent. PLoS One **6:**e25464. http://dx.doi.org/10.1371/journal.pone.0025464.
17. **Clement C, Tiwari V, Scanlan PM, Valyi-Nagy T, Yue BY, Shukla D.** 2006. A novel role for phagocytosis-like uptake in herpes simplex virus entry. J Cell Biol **174:**1009–1021. http://dx.doi.org/10.1083/jcb.200509155.
18. **Gianni T, Campadelli-Fiume G.** 2012. alphaVbeta3-integrin relocalizes nectin1 and routes herpes simplex virus to lipid rafts. J Virol **86:**2850–2855. http://dx.doi.org/10.1128/JVI.06689-11.
19. **Davison AJ, Eberle R, Ehlers B, Hayward GS, McGeoch DJ, Minson AC, Pellett PE, Roizman B, Studdert MJ, Thiry E.** 2009. The order Herpesvirales. Arch Virol **154:**171–177. http://dx.doi.org/10.1007/s00705-008-0278-4.
20. **Roizman B** 1996. Herpesviridae, p 2221–2230. *In* Fields BN, Knipe DM, Howley PM, Channock RM, Melnick JL, Monath TP, Roizman B, Straus SE (ed), Fields virology, 3rd ed. Lippincott Raven, Philadelphia, PA.
21. **Kurtz BM, Singletary LB, Kelly SD, Frampton AR, Jr.** 2010. Equus caballus major histocompatibility complex class I is an entry receptor for equine herpesvirus type 1. J Virol **84:**9027–9034. http://dx.doi.org/10.1128/JVI.00287-10.
22. **Azab W, Lehmann MJ, Osterrieder N.** 2013. Glycoprotein H and alpha4beta1 integrins determine the entry pathway of alphaherpesviruses. J Virol **87:**5937–5948. http://dx.doi.org/10.1128/JVI.03522-12.
23. **Cheshenko N, Liu W, Satlin LM, Herold BC.** 2005. Focal adhesion kinase plays a pivotal role in herpes simplex virus entry. J Biol Chem **280:**31116–31125. http://dx.doi.org/10.1074/jbc.M503518200.
24. **Kerur N, Veettil MV, Sharma-Walia N, Sadagopan S, Bottero V, Paul AG, Chandran B.** 2010. Characterization of entry and infection of monocytic THP-1 cells by Kaposi's sarcoma associated herpesvirus (KSHV): role of heparan sulfate, DC-SIGN, integrins and signaling. Virology **406:**103–116. http://dx.doi.org/10.1016/j.virol.2010.07.012.
25. **Krishnan HH, Sharma-Walia N, Streblow DN, Naranatt PP, Chandran B.** 2006. Focal adhesion kinase is critical for entry of Kaposi's sarcoma-associated herpesvirus into target cells. J Virol **80:**1167–1180. http://dx.doi.org/10.1128/JVI.80.3.1167-1180.2006.
26. **Giancotti FG, Ruoslahti E.** 1999. Integrin signaling. Science **285:**1028–1032. http://dx.doi.org/10.1126/science.285.5430.1028.
27. **Kanner SB, Grosmaire LS, Ledbetter JA, Damle NK.** 1993. Beta 2-integrin LFA-1 signaling through phospholipase C-gamma 1 activation. Proc Natl Acad Sci U S A **90:**7099–7103. http://dx.doi.org/10.1073/pnas.90.15.7099.
28. **Sekiya F, Poulin B, Kim YJ, Rhee SG.** 2004. Mechanism of tyrosine phosphorylation and activation of phospholipase C-gamma 1. Tyrosine 783 phosphorylation is not sufficient for lipase activation. J Biol Chem **279:**32181–32190. http://dx.doi.org/10.1074/jbc.M405116200.
29. **Kato A, Yamamoto M, Ohno T, Kodaira H, Nishiyama Y, Kawaguchi Y.** 2005. Identification of proteins phosphorylated directly by the Us3 protein kinase encoded by herpes simplex virus 1. J Virol **79:**9325–9331. http://dx.doi.org/10.1128/JVI.79.14.9325-9331.2005.
30. **Van Seventer GA, Bonvini E, Yamada H, Conti A, Stringfellow S, June CH, Shaw S.** 1992. Costimulation of T cell receptor/CD3-mediated activation of resting human $CD4^+$ T cells by leukocyte function-associated antigen-1 ligand intercellular cell adhesion molecule-1 involves prolonged inositol phospholipid hydrolysis and sustained increase of intracellular Ca2+ levels. J Immunol **149:**3872–3880.
31. **Rhee SG.** 2001. Regulation of phosphoinositide-specific phospholipase C. Annu Rev Biochem **70:**281–312. http://dx.doi.org/10.1146/annurev.biochem.70.1.281.
32. **Berridge MJ.** 1993. Inositol trisphosphate and calcium signalling. Nature **361:**315–325. http://dx.doi.org/10.1038/361315a0.
33. **Zhou Y, Frey TK, Yang JJ.** 2009. Viral calciomics: interplays between Ca2+ and virus. Cell Calcium **46:**1–17. http://dx.doi.org/10.1016/j.ceca.2009.05.005.
34. **Hay JC.** 2007. Calcium: a fundamental regulator of intracellular membrane fusion? EMBO Rep **8:**236–240. http://dx.doi.org/10.1038/sj.embor.7400921.
35. **Berridge MJ, Bootman MD, Roderick HL.** 2003. Calcium signalling: dynamics, homeostasis and remodelling. Nat Rev Mol Cell Biol **4:**517–529. http://dx.doi.org/10.1038/nrm1155.
36. **Mikoshiba K, Hattori M.** 2000. IP3 receptor-operated calcium entry. Sci STKE **2000:**E1.
37. **Cheshenko N, Del Rosario B, Woda C, Marcellino D, Satlin LM, Herold BC.** 2003. Herpes simplex virus triggers activation of calcium-signaling pathways. J Cell Biol **163:**283–293. http://dx.doi.org/10.1083/jcb.200301084.
38. **Cheshenko N, Trepanier JB, Stefanidou M, Buckley N, Gonzalez P, Jacobs W, Herold BC.** 2013. HSV activates Akt to trigger calcium release and promote viral entry: novel candidate target for treatment and suppression. FASEB J **27:**2584–2599. http://dx.doi.org/10.1096/fj.12-220285.
39. **Azab W, Zajic L, Osterrieder N.** 2012. The role of glycoprotein H of equine herpesviruses 1 and 4 (EHV-1 and EHV-4) in cellular host range and integrin binding. Vet Res **43:**61. http://dx.doi.org/10.1186/1297-9716-43-61.
40. **Moriuchi M, Moriuchi H, Williams R, Straus SE.** 2000. Herpes simplex virus infection induces replication of human immunodeficiency virus type 1. Virology **278:**534–540. http://dx.doi.org/10.1006/viro.2000.0667.
41. **Foskett JK, White C, Cheung K-, Mak DD.** 2007. Inositol trisphosphate receptor Ca2+ release channels. Physiol Rev **87:**593–658. http://dx.doi.org/10.1152/physrev.00035.2006.
42. **Huang T, Lehmann MJ, Said A, Ma G, Osterrieder N.** 2014. Major histocompatibility complex class I downregulation induced by equine herpesvirus type 1 pUL56 is through dynamin-dependent endocytosis. J Virol **88:**12802–12815. http://dx.doi.org/10.1128/JVI.02079-14.
43. **Cao H, Thompson HM, Krueger EW, McNiven MA.** 2000. Disruption of Golgi structure and function in mammalian cells expressing a mutant dynamin. J Cell Sci **113:**1993–2002.
44. **Bevers EM, Williamson PL.** 2010. Phospholipid scramblase: an update. FEBS Lett **584:**2724–2730. http://dx.doi.org/10.1016/j.febslet.2010.03.020.
45. **Berghold VM, Gauster M, Hemmings DG, Moser G, Kremshofer J, Siwetz M, Sundl M, Huppertz B.** 2015. Phospholipid scramblase 1 (PLSCR1) in villous trophoblast of the human placenta. Histochem Cell Biol **143:**381–396. http://dx.doi.org/10.1007/s00418-014-1294-y.
46. **Dekkers DW, Comfurius P, Vuist WM, Billheimer JT, Dicker I, Weiss HJ, Zwaal RF, Bevers EM.** 1998. Impaired Ca2+-induced tyrosine phosphorylation and defective lipid scrambling in erythrocytes from a patient with Scott syndrome: a study using an inhibitor for scramblase that mimics the defect in Scott syndrome. Blood **91:**2133–2138.
47. **Gonzalez LJ, Gibbons E, Bailey RW, Fairbourn J, Nguyen T, Smith SK, Best KB, Nelson J, Judd AM, Bell JD.** 2009. The influence of membrane physical properties on microvesicle release in human erythrocytes. PMC Biophys **2:**7. http://dx.doi.org/10.1186/1757-5036-2-7.
48. **Eitzen G.** 2003. Actin remodeling to facilitate membrane fusion. Biochim Biophys Acta **1641:**175–181. http://dx.doi.org/10.1016/S0167-4889(03)00087-9.
49. **Iyengar S, Hildreth JE, Schwartz DH.** 1998. Actin-dependent receptor colocalization required for human immunodeficiency virus entry into host cells. J Virol **72:**5251–5255.
50. **Pontow SE, Heyden NV, Wei S, Ratner L.** 2004. Actin cytoskeletal reorganizations and coreceptor-mediated activation of rac during human immunodeficiency virus-induced cell fusion. J Virol **78:**7138–7147. http://dx.doi.org/10.1128/JVI.78.13.7138-7147.2004.
51. **Dushek O, Mueller S, Soubies S, Depoil D, Caramalho I, Coombs D,**

**Valitutti S.** 2008. Effects of intracellular calcium and actin cytoskeleton on TCR mobility measured by fluorescence recovery. PLoS One **3:**e3913. http://dx.doi.org/10.1371/journal.pone.0003913.
52. **Keay S, Baldwin BR, Smith MW, Wasserman SS, Goldman WF.** 1995. Increases in [Ca2+]I mediated by the 92.5-kDa putative cell membrane receptor for HCMV gp86. Am J Physiol **269:**C11–C21.
53. **Cheshenko N, Liu W, Satlin LM, Herold BC.** 2007. Multiple receptor interactions trigger release of membrane and intracellular calcium stores critical for herpes simplex virus entry. Mol Biol Cell **18:**3119–3130. http://dx.doi.org/10.1091/mbc.E07-01-0062.
54. **Cheshenko N, Trepanier JB, Gonzalez PA, Eugenin EA, Jacobs WR, Jr, Herold BC.** 2014. Herpes simplex virus type 2 glycoprotein H interacts with integrin $\alpha v\beta 3$ to facilitate viral entry and calcium signaling in human genital tract epithelial cells. J Virol **88:**10026–10038. http://dx.doi.org/10.1128/JVI.00725-14.
55. **Manninen A, Saksela K.** 2002. HIV-1 Nef interacts with inositol trisphosphate receptor to activate calcium signaling in T cells. J Exp Med **195:**1023–1032. http://dx.doi.org/10.1084/jem.20012039.
56. **Benali-Furet NL, Chami M, Houel L, De Giorgi F, Vernejoul F, Lagorce D, Buscail L, Bartenschlager R, Ichas F, Rizzuto R, Paterlini-Bréchot P.** 2005. Hepatitis C virus core triggers apoptosis in liver cells by inducing ER stress and ER calcium depletion. Oncogene **24:**4921–4933. http://dx.doi.org/10.1038/sj.onc.1208673.
57. **Tian P, Estes MK, Hu Y, Ball JM, Zeng CQ, Schilling WP.** 1995. The rotavirus nonstructural glycoprotein NSP4 mobilizes Ca2+ from the endoplasmic reticulum. J Virol **69:**5763–5772.
58. **Bozym RA, Morosky SA, Kim KS, Cherry S, Coyne CB.** 2010. Release of intracellular calcium stores facilitates coxsackievirus entry into polarized endothelial cells. PLoS Pathog **6:**e1001135. http://dx.doi.org/10.1371/journal.ppat.1001135.
59. **Mogami H, Lloyd Mills C, Gallacher DV.** 1997. Phospholipase C inhibitor, U73122, releases intracellular Ca2+, potentiates ins(1,4,5)P3-mediated Ca2+ release and directly activates ion channels in mouse pancreatic acinar cells. Biochem J **324:**645–651. http://dx.doi.org/10.1042/bj3240645.
60. **Oka T, Sato K, Hori M, Ozaki H, Karaki H.** 2002. Xestospongin C, a novel blocker of IP3 receptor, attenuates the increase in cytosolic calcium level and degranulation that is induced by antigen in RBL-2H3 mast cells. Br J Pharmacol **135:**1959–1966. http://dx.doi.org/10.1038/sj.bjp.0704662.
61. **De Smet PD, Parys JB, Callewaert G, Weidema AF, Hill E, De Smedt HD, Erneux C, Sorrentino V, Missiaen L.** 1999. Xestospongin C is an equally potent inhibitor of the inositol 1,4,5-trisphosphate receptor and the endoplasmic-reticulum Ca(2+) pumps. Cell Calcium **26:**9–13. http://dx.doi.org/10.1054/ceca.1999.0047.
62. **Osterrieder N.** 1999. Construction and characterization of an equine herpesvirus 1 glycoprotein C negative mutant. Virus Res **59:**165–177. http://dx.doi.org/10.1016/S0168-1702(98)00134-8.
63. **Azab W, Osterrieder N.** 2012. Glycoproteins D of equine herpesvirus type 1 (EHV-1) and EHV-4 determine cellular tropism independently of integrins. J Virol **86:**2031–2044. http://dx.doi.org/10.1128/JVI.06555-11.
64. **Rawat SS, Viard M, Gallo SA, Rein A, Blumenthal R, Puri A.** 2003. Modulation of entry of enveloped viruses by cholesterol and sphingolipids. Mol Membr Biol **20:**243–254. http://dx.doi.org/10.1080/0968768031000104944.
65. **Bretscher MS.** 1972. Asymmetrical lipid bilayer structure for biological membranes. Nat New Biol **236:**11–12. http://dx.doi.org/10.1038/newbio236011a0.
66. **Zhou Q, Zhao J, Stout JG, Luhm RA, Wiedmer T, Sims PJ.** 1997. Molecular cloning of human plasma membrane phospholipid scramblase. A protein mediating transbilayer movement of plasma membrane phospholipids. J Biol Chem **272:**18240–18244. http://dx.doi.org/10.1074/jbc.272.29.18240.
67. **Coil DA, Miller AD.** 2005. Enhancement of enveloped virus entry by phosphatidylserine. J Virol **79:**11496–11500. http://dx.doi.org/10.1128/JVI.79.17.11496-11500.2005.
68. **Zaitseva E, Yang S, Melikov K, Pourmal S, Chernomordik LV.** 2010. Dengue virus ensures its fusion in late endosomes using compartment-specific lipids. PLoS Pathog **6:**e1001131. http://dx.doi.org/10.1371/journal.ppat.1001131.
69. **DuBois RM, Vaney M, Tortorici MA, Kurdi RA, Barba-Spaeth G, Krey T, Rey FA.** 2013. Functional and evolutionary insight from the crystal structure of rubella virus protein E1. Nature **493:**552–556. http://dx.doi.org/10.1038/nature11741.
70. **Dubé M, Rey FA, Kielian M.** 2014. Rubella virus: first calcium-requiring viral fusion protein. PLoS Pathog **10:**e1004530. http://dx.doi.org/10.1371/journal.ppat.1004530.
71. **Heldwein EE, Lou H, Bender FC, Cohen GH, Eisenberg RJ, Harrison SC.** 2006. Crystal structure of glycoprotein B from herpes simplex virus 1. Science **313:**217–220. http://dx.doi.org/10.1126/science.1126548.
72. **Dimitrov DS, Broder CC, Berger EA, Blumenthal R.** 1993. Calcium ions are required for cell fusion mediated by the CD4$^-$ human immunodeficiency virus type 1 envelope glycoprotein interaction. J Virol **67:**1647–1652.
73. **Masuda A, Goshima K.** 1980. The role of extracellular calcium ions in HVJ (Sendai virus)-induced cell fusion. Biochim Biophys Acta **599:**596–609. http://dx.doi.org/10.1016/0005-2736(80)90203-5.
74. **Rudolph J, O'Callaghan DJ, Osterrieder N.** 2002. Cloning of the genomes of equine herpesvirus type 1 (EHV-1) strains KyA and racL11 as bacterial artificial chromosomes (BAC). J Vet Med B Infect Dis Vet Public Health **49:**31–36. http://dx.doi.org/10.1046/j.1439-0450.2002.00534.x.
75. **Azab W, Kato K, Arii J, Tsujimura K, Yamane D, Tohya Y, Matsumura T, Akashi H.** 2009. Cloning of the genome of equine herpesvirus 4 strain TH20p as an infectious bacterial artificial chromosome. Arch Virol **154:**833–842. http://dx.doi.org/10.1007/s00705-009-0382-0.
76. **Distler JHW, Jungel A, Kurowska-Stolarska M, Michel BA, Gay RE, Gay S, Distler O.** 2005. Nucleofection: a new, highly efficient transfection method for primary human keratinocytes. Exp Dermatol **14:**315–320. http://dx.doi.org/10.1111/j.0906-6705.2005.00276.x.
77. **Pietiainen V, Marjomaki V, Upla P, Pelkmans L, Helenius A, Hyypia T.** 2004. Echovirus 1 endocytosis into caveosomes requires lipid rafts, dynamin II, and signaling events. Mol Biol Cell **15:**4911–4925. http://dx.doi.org/10.1091/mbc.E04-01-0070.